THE UNIVERSITY OF QUEENSLAND

Master of Engineering Thesis

The recyclability of lithium-ion battery materials

Student Name: Phuc Anh LE

Course Code: ENGG7282

Supervisor: Dr. Ruth Knibbe

Submission date: 30 May 2019

A thesis submitted in partial fulfilment of the requirements of the Master of Engineering degree in Chemical Engineering

UQ Engineering

Faculty of Engineering, Architecture and Information Technology

ACKNOWLEDGEMENTS

For acknowledgement, I personally would like to express my in-depth and truly gratitude to these following individuals that this accomplishment would not be feasible without their support.

First of all, I express my deepest appreciation to my supervisor Dr. Ruth Knibbe for giving me precious chance to join in this project. Her valuable guidance, advices as well as comprehensive knowledge underpin for my personal development as well as the completion of this thesis report. I have learnt many things from her after this project, which are not only knowledge regarding the project but also about time management, organization and problem approaching.

Secondly, I must give my gratitude to Ming Li and Lingbing Ran for their valuable supports through laboratory conductions as well as running tests for my samples. I most appreciate your tireless help during my thesis execution.

I would also like to acknowledge James Gudgeon from hydrometallurgy lab. Without his dedicated helps and advices, I cannot complete my experiments successfully in this thesis.

Finally, to my family and my wife, you should know that your priceless encouragement and support are worth much more than I can express on this report.

ABSTRACT

Lithium-ion batteries (LIBs) have been extensively applied as the electrochemical power source in portable electronic devices, energy storage systems and electric vehicles. LIBs are the battery technology having the highest development during the last decade. LIBs market is also predicted counting 70% in 112 billion USD by 2025. Subsequently, there is also a huge number of spent LIBs released annually. The current processes for recycling spent LIBs waste highly valuable components and only recovers the spent LIBs as cheap products. This results in only 5% of spent LIBs current recycled due to high cost and low profit of recycling. The continuity of current situation could lead to the hindrance of LIBs development due to environmental issues. Therefore, an effective recycling scheme for recovering highly valuable components (i.e. lithium, cobalt) is necessary.

The cathode of LIBs is the determinant component for the battery performance. This is also most valuable component because it contains highly valuable metals such as lithium and cobalt. Hence, this thesis focuses on recycling lithium and cobalt from the cathode of spent LIBs by hydrometallurgical recycling scheme. It includes the optimization of acid leaching stage, selective precipitation of key metals from leaching solution, synthesis of LCO from precipitate and fabrication of new battery from recycled product.

This research has figured out that the optimal acid leaching can be achieved by using 3 M H_2SO_4 with 4 wt% H_2O_2 in 2 hours at 60 ^oC and 20 g/L pulp density. The optimal acid leaching stage provides over 99% leaching efficiency of lithium and cobalt from LCO of spent LIBs. By using NaOH and Na_2CO_3, 29.07% and 87.49% of lithium and cobalt were recovered from the leaching solution. However, they were a mixture of hydroxides rather than separated precipitates.

The precipitated product was then calcined to form LCO through solid-state reaction between lithium and cobalt hydroxides. The XRD result of recycled sample after calcination shows high similarity to the XRD pattern of standard LCO. However, comparing to XRD result of commercial LCO powder, the intensity of peaks in recycled LCO XRD are lower than peak intensity of commercial LCO XRD. This can result from the presence of impurities as well as low yield of LCO in the recycled LCO sample.

The recycled LCO sample was then used as cathodic material for fabrication of new LIB coin cell. The fabricated recycled LCO battery shows a similar electrolyte resistance and

charge transfer characteristic but unfortunately a poor battery performance comparing to the assembled commercial LCO battery. The commercial LCO battery has initial capacity of approximately 120 $mAh.g^{-1}$, which decays to approximately 85 $mAh.g^{-1}$ after 37 cycles. The recycled LCO battery has a low irreversible specific capacity (6.7 $mAh.g^{-1}$) and rapidly faded to 0.4 $mAh.g^{-1}$ after only 3 cycles. The major root causes for this are the presence of impurities as well as low yield of LCO formation in recycled LCO. They inhibit the intercalation/de-intercalation of lithium ions to cathodic material, which is basic requirement for LIB operation.

Overall, these following points are recommended for further progress of the project.

- Diversifying of spent LIBs source by recycling spent LIBs from laptop, camera, other smartphone brands (e.g. Samsung, Oppo);
- Researching for a low-concentrated leaching medium with similar leaching efficiency;
- Studying a combination of solvent extraction and selective precipitation for metal recovery from leaching solution;
- Higher number of cycles at different charge/discharge rate in cycling performance tests for in-depth evaluation of recycled product.

TABLE OF CONTENT

LIST OF TABLES

LIST OF FIGURES

ACRONYMS AND ABBREVIATIONS

AAS	Atomic absorption spectroscopy
D2EHPA	Di-(2-ethylhexyl)-phosphoric acid
DEC	Diethyl carbonate
DMSO	Dimethyl sulfoxide
EIS	Electrochemical Impedance Spectroscopy
EDS	Energy dispersive spectroscopy
ESS	Energy Storage System
EVs	Electric vehicles
HEVs	Hybrid electric vehicles
LCO	Lithium Cobalt Oxide
LFP	Lithium Iron Phosphate
LIBs	Lithium-ion batteries
LMO	Lithium Manganese Oxide
LTO	Lithium Titanium Oxide
NCA	Lithium Nickel Cobalt Aluminium Oxide
NiCd battery	Nickel–cadmium battery
NiMH battery	Nickel–metal hydride battery
NMC	Lithium Nickel Manganese Cobalt Oxide
P507	2-Ethylhexyl 2-Ethylhexyl Phosphate
PC	Propylene carbonate
PC-88A	2-ethyl hexyl phosphonic acid mono-2-ethyl hexyl ester
PE	Polyethylene
PHEVs	Plug-in hybrid electric vehicles
PP	Polypropylene
SEM	Scanning electron microscopy
TEM	Transmission electron microscopy
XRD	X-ray Powder Diffraction (XRD)

1 INTRODUCTION

1.1 Background

Over the past few years, the world is launching globally a trend for environment protection to reach sustainability. Fossil fuels, which have been serving our society energy demands since ancient time, gradually exhibit many negative influences for environment as well as energy security due to their price instability. As a result, numerous companies are currently investing resources to develop electric vehicles and equipment powered by energy storage sources instead of traditional internal combustion engine vehicles/equipment. Hence, they can isolate themselves from fossil fuel price instability. In addition, recent decades are also witnessing a significantly increasing need for portable electronic devices (e.g. smartphones, tablets, laptops, etc.), which are also powered by electric storage systems – batteries.

These factors result in the emergence and proliferation of many different types of energy storage systems, such as lithium-ion battery (LIB), nickel-metal hydride battery (NiMH), standard lead-acid battery or nickel-cadmium battery (NiCd) [1]. Among them, the LIBs are popularly known and used due to its excellent performance in terms of energy, power density and enduring stability.

Since its first commercial appearance by the Sony Corporation in 1990s, LIBs have been widely utilized in portable electronic devices, energy systems and electric equipment/vehicles [2]. The LIB market expanded from only 9 billion U$ in 2005 up to approximately 45 billion U$ in 2016 with a major proportion of application in electronic device [3]. In 2025, this promising market is expected to achieve approximately 80 billion U$ making up 70% of rechargeable battery market (Figure 1.1).

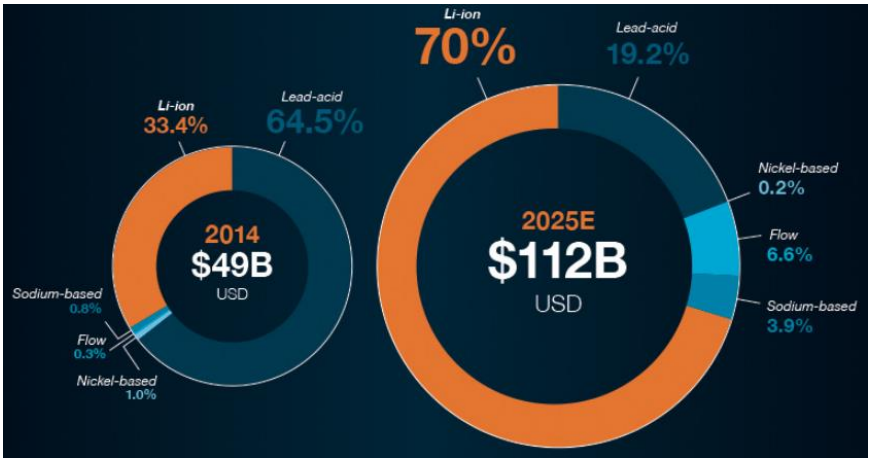

Figure 1.1 – Rechargeable battery market size (Source: [4])

1.2 Motivation for LIB recycling

The above prediction for LIB proliferation is currently being impeded because of raw material scarcity as well as environment problems from spent LIBs. Landfilling is conventional method for treating spent LIBs. Nevertheless, it may cause hazardous risks for environment and human health due to presence of heavy metals and organic electrolyte in LIB. In upcoming years, when the LIBs amount increases significantly to meet demands, these issues become non-negligible due to corresponding huge quantity of spent LIBs. From 2000 to 2010, The United Nations estimated a total manufacturing of 768.9 million digital cameras, 12.7 billion mobile phones and 94.4 million laptops, which require a significant amount of powering LIBs [5]. As a result, a huge discarding of spent LIBs is unavoidable from these end-of-life electronic equipment. It is predicted a release of 25 billion spent LIBs – equivalent to a mass of 500,000 tons of them only from China by 2020 and exponentially increase over years [6]. However, only approximately 5% of spent LIBs are currently recycled [7], this means current processes for recycling are not sufficient to handle disposed LIBs amount and continuously increasing quantity in the future.

In addition, there are some valuable elements in spent LIBs, particularly in cathode, such as lithium, cobalt and nickel (i.e. comprises approximately 5-7 wt% lithium and 5-20 wt% cobalt in two electrodes). These components have high economic benefits because of their wide applications (e.g. lithium can be used in psychological disorder medicine and cobalt is required in super alloys, aircraft engines and magnets, etc.) [6, 8]. Cobalt has a commercial price of over 75,000 $/t, which is much higher than any other important metals for industries and manufacturing such as nickel, manganese, copper, aluminium (Figure 1.2), or molybdenum (~26,000 $/t) and tin (~21,000 $/t) [9]. Therefore, it would create significant economic benefit if cobalt could be recycled from cathode materials of spent LIBs and then used for producing new LIBs as well as other applications as mentioned above.

Moreover, cobalt is also evaluated as in critical state of supply risk (Figure 1.3). This is because cobalt can only be exploited as a by-product of nickel and copper mining process. In addition, 65% supplies of cobalt come from Democratic Republic of Congo, and Zambia. The risks from political instability and deeply-rooted corruption of these countries can cause scarcity issue unpredictably. In addition, the ethical practices of cobalt mining in these countries are also doubtfully questioned over years [6]. From Figure 1.3, it can be seen that lithium is also locating in a close position to critical state area. This metal has medium

economic importance though, its supply risk is gradually reaching the critical state area due to its increasing need and consumption, especially in LIBs [10].

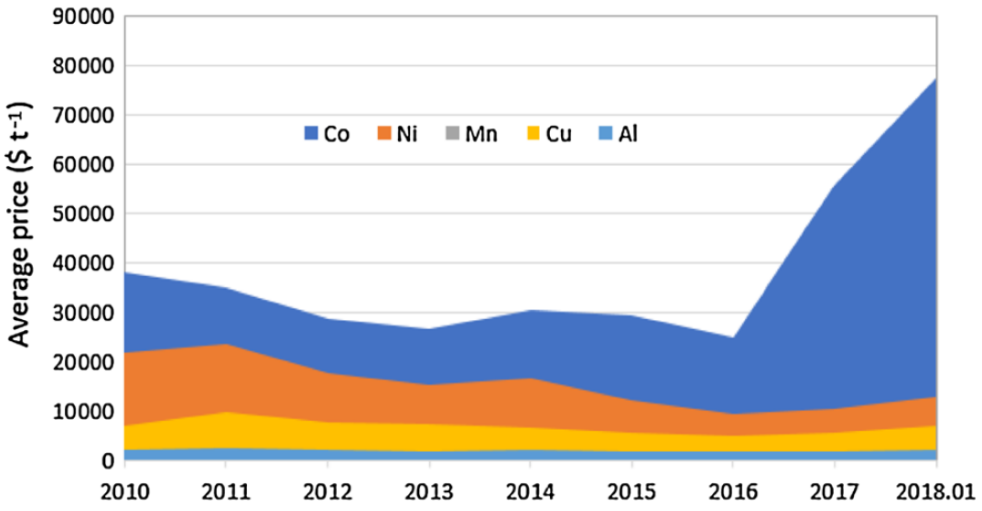

Figure 1.2 – Average prices of common metals in manufacturing and industries (Source: [11])

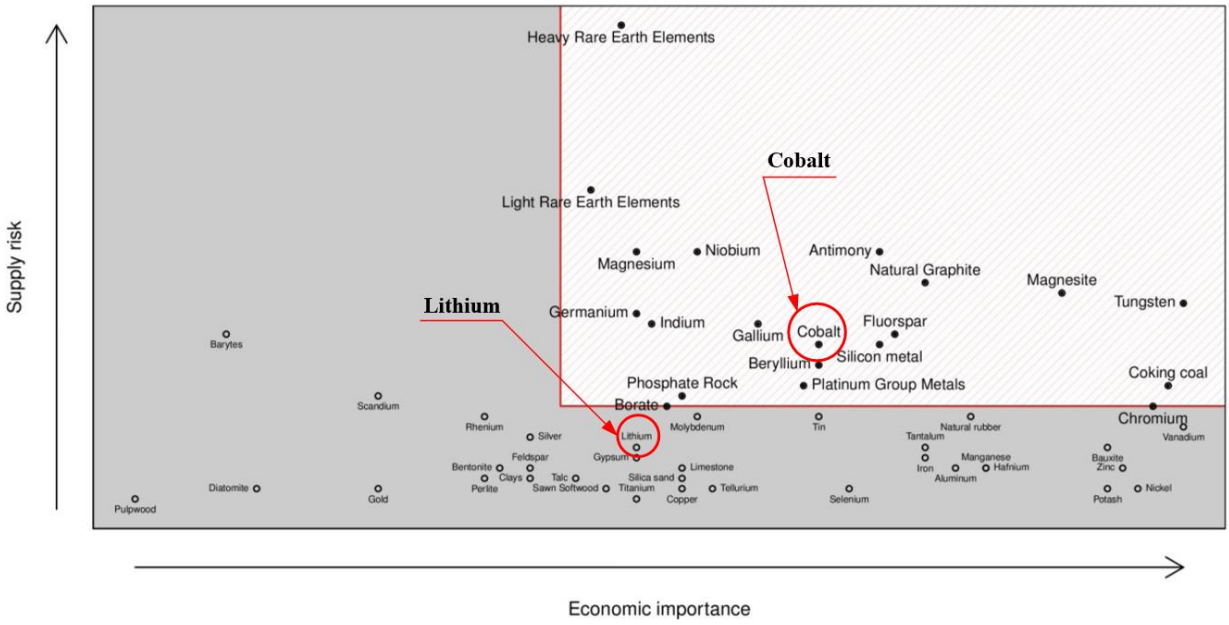

Figure 1.3 – EU criticality assessment of raw materials (Source: [10])

Overall, current treating method for spent LIBs – landfilling – can result in many significant threats for human health and environment in terms of fire/explosion, leakages of hazardous elements (e.g. heavy metals, organic electrolytes), especially when spent LIB quantity increases in upcoming years. That drawback together with the high economic value of components (i.e. lithium, cobalt) in spent LIBs cathode as well as their high supply risks

necessitate a proper recycling scheme for spent LIBs to protect human health and environment as well as proceed LIB market development.

1.3 Aims and tasks

The thesis focuses on developing a methodology for recycling LCO (i.e. a popular type of LIB) cathode material and producing a new battery cell from the recycled. The aim can be achieved by completing these following tasks

1. Accomplish a LIB literature review to understand
   - The LIB market;
   - LIB recycling area;
   - Industry-scale schemes/processes for recycling spent LIB;
   - Methodology and step-by-step study for spent LIBs treatment.
2. Complete a laboratory scheme for acid leaching;
3. Conducting experiment to understand how leaching conditions affect acid leaching efficiency.
4. Develop a selective precipitation method to separate effectively cobalt from leachate solution;
5. Produce new cathode from recycled metals and then fabricate a new LIB using this cathode.

2 LITERATURE REVIEW

Before initiating a laboratory scheme for recycling the spent LIBs, a comprehensive review is necessary to highlight the historical development, the current chemistries of battery components as well as market trends of lithium-ion batteries. In addition, a brief overview in terms of laboratory and industrial spent LIB recycling is also crucial to provide basic understanding, direction for forming step-by-step treatment for spent LIBs in this thesis. Last but not least, basic knowledges regarding analytical techniques, which are used in this spent LIBs recycling study, are also briefly introduced. These contents are all covered in this Literature Review as providing initial understandings and basis for the subsequent engineering contents with regard to recycling spent LIBs.

2.1 Lithium-ion batteries

2.1.1 Historic review

In the 1970s, the first lithium batteries was constructed by Michael Stanley Whittingham, who employed lithium and titanium sulphide for battery electrodes [12]. This chemistry

discover was not useful but still paved the way for further works and breakthrough. The next generation of reversible intercalation electrode batteries was discovered by Jürgen Otto Besenhard [13, 14]. Samar Basu then uncovered lithium electrochemical intercalation in graphite [15]. Rachid Yazami then solved the problem in terms of rapid deterioration of battery cell assembled that time through his research regarding reversible intercalation of lithium ion in graphite in the early 1980s [16]. After that, many efforts and research was conducted by numerous academic groups to develop lithium-ion batteries, especially cathode materials [1]. Until 1991, lithium-ion batteries had its commercial breakthrough by the Sony Corporation to power their handheld video cameras [17]. And this has initiated for rapid development and application expansion of this battery type up to now.

2.1.2 Lithium ion battery components

A typical lithium-ion battery includes four major components: anode, cathode, electrolyte and separator. The variation of these component material results in significant impact on crucial characteristics of a lithium-ion battery performance, which are energy density, durability, cycle life and safety.

2.1.2.1 Cathode material

A LIB cathode is produced by coating foil of aluminium current collector with active cathode material. Cathode play an important role in commercial LIBs because it contains valuable metals (e.g. cobalt, lithium, manganese) and also determine battery properties as well as performance. Therefore, commercial lithium-ion batteries are commonly named by their active cathode material, which is the lithium-ion donator in battery [1]. LCO is the most popular active material for cathode, however, its market proportion gradually reduce due to the presence of other cathode materials, especially NMC and NCA (Table 2.1 and Figure 2.1). These new active cathode materials have impressive electrochemical properties and widely applied including in electric vehicles (Table 2.2).

Table 2.1 – Global market of LIB active cathode materials (Source: [18])

Year	$LiNi_{0.33}Mn_{0.33}Co_{0.33}O_2$ (NMC) (%)	$LiCoO_2$ (LCO) (%)	$LiMn_2O_4$ (LMO) (%)	$LiFePO_4$ (LFP) (%)	$LiNiCoAlO_2$ (NCA) (%)
2008	18.9	60.8	10.5	3.5	6.5
2012	29.0	37.2	21.4	5.2	7.2
2014	31.0	39.8	15.9	8.8	4.5

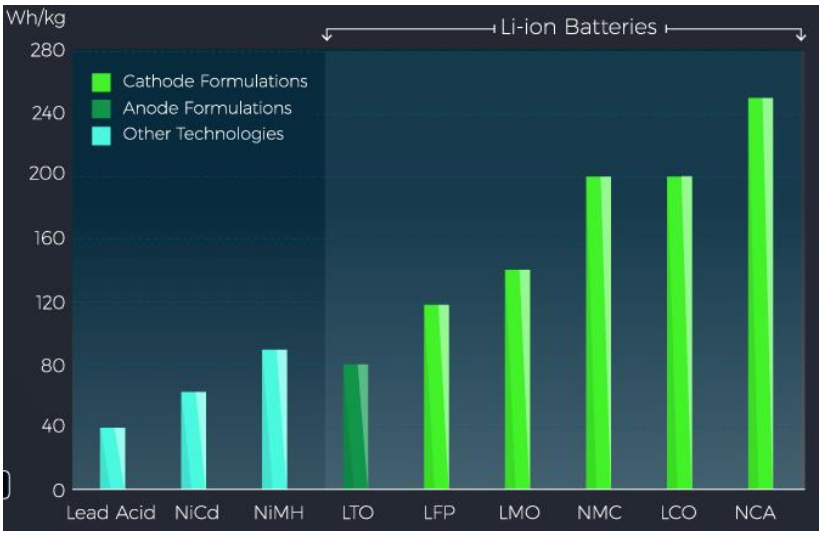

Figure 2.1 – 2017 battery options
(Source: [19])

Table 2.2 – LIB cathode materials and their applications
(Source: [1, 20])

Name	Advantages	Disadvantages	Application
LCO	• High energy density (150–190 Wh/kg); • Maturity of technology; • Acceptable durability (~1000 full cycle lives).	• Low safety inherence (low temperature of thermal runaway – 150 °C); • Resource availability.	Small portable electronic devices (e.g. laptop, smartphone, tablet)
LMO	• Improved durability (1000-1500 cycle lives); • Safer inherent (thermal runaway occurs at 250 °C); • Low internal resistance; • Abundance of eco-friendly raw materials.	• Low specific energy (100-140 Wh/kg); • Low energy capacity resulting from spinel structure.	Medical devices, power tools, e-bikes
LFP	• Good durability; • Higher safety level; • Abundance of eco-friendly raw materials; • Enhanced durability (2000 full cycle lives); • Wide range of state of charge.	• Low energy density (90-140 Wh/kg); • High cost due to youth technology.	Power storage, power supply systems for both grid connection and off-grid.
NCA	• Moderate reliance on cobalt; • Excellent energy density (200-250 Wh/kg); • Good durability (1000-1500 cycle lives);	• Relatively high cost due to dependence on nickel and cobalt; • Raw material availability (Cobalt).	Major applications in electric vehicles (EVs), grid connection (e.g. loadshift or backup).
NMC	• Good specific energy (140-200 Wh/kg); • Long durability (1000-2000 cycle lives); • Mature technology;	• Reliance on cobalt; • Patent issues.	Medical devices, portable devices, power tools, electric vehicles (EVs) and plug-in hybrid electric vehicles (PHEVs).

2.1.2.2 Anode material

Anode manufacturing process is similar to its cathode but the anode material is coated on cooper current collector foil. Since commercial production of LIBs in the 1990s, graphite and hard carbon have been used as anode materials. Over time, graphite still sustain the dominance in anode market over hard carbon due to this material superior profile of discharge [21].

However, graphite has recently revealed some weaknesses that can impede commercial and sustainable development of LIBs. Firstly, it virtually achieves its optimal theoretical capacity density (~372 mAh/g equivalent to approximate 150 Wh/kg energy density), which is inadequate to satisfy energy density requirement of electric vehicles [22]. In addition, graphite has an inherent irreversible that contributes to lithium dendrite growth as the LIBs are cycled with high C-rate [23]. For those reasons, many LIBs manufacturers have launched researching for non-graphite anode such as silicon, tin or spinel lithium titanate ($Li_4Ti_5O_{12}$ – LTO) [1, 22, 23]. LTO is easy to improve as well as adjust its electrochemical properties through fine-tuning its nanostructure [22].

2.1.2.3 Electrolyte solution

Electrolyte solution has a key role in any cell operation because it facilitates movement of ions (i.e. lithium ions for LIBs) between electrodes that generate electric current. In LIBs, the electrolyte is a mixture of organic solvents and lithium salts. Common organic solvents are dimethyl-carbonate, ethyl-methyl-carbonate, propylene carbonate (PC), dimethyl sulfoxide (DMSO) and diethyl carbonate (DEC) [6]. Lithium-hexafluoroarsenate ($LiAsF_6$), lithium-perchlorate ($LiClO_4$) and lithium-hexafluorophosphate ($LiPF_6$), Lithium tetrafluoroborate ($LiBF_4$) are popular lithium salts [24].

2.1.2.4 Separator

The lithium-ion battery separator, which is commonly constructed from polyolefin, is a microporous membrane. The separator is immersed in electrolyte solution and placed between anode and cathode, as a safety component to prevent short-circuiting when two electrodes contact directly. The lithium ion permeability of this membrane exclusively allows flow of charged particles -lithium ions -between two electrodes and consequently guarantee normal operation of battery. LIB separator can be multi-layer or a single layer that made of polypropylene (PP) or polyethylene (PE) [6].

Overall, all of these components play important roles for determination of battery performance and properties. Any modification of them, hence, can result in improvement of battery properties and operation. Among these components, electrodes, especially cathode, are exceptionally important because they can directly affect LIB characteristics (e.g. safety, charging time, depth of discharge, capacity, etc.). Therefore, in order to achieve a comprehensive knowledge of LIB cycle life, optimization and recycling attempts have been initiated to develop this potential battery effectively and sustainably.

2.1.3 Working mechanism

The LIB operation – charging and discharging processes – is based on intercalation/de-intercalation reactions of lithium ions between two electrodes [25]. When an ions or molecule is included or inserted to a crystal lattice or layered structure, the intercalation reaction occurs. In a LIB system, two electrodes operate as solid host networks that can store and release lithium ions as well as electron during battery operation.

During discharging, lithium ions are de-intercalated and move with electrons from anode to cathode. The movement of electron through external circuit generates electric current and electrical power. These transferred particles – lithium ions and electrons – are then intercalated to layered structure of cathode material. These electrochemical reactions are reversible, hence, as applying an external electric current to a LIB, a reverse process happens. Figure 2.2 schematically describes electrochemical reactions of an LCO-graphite LIB during its operation.

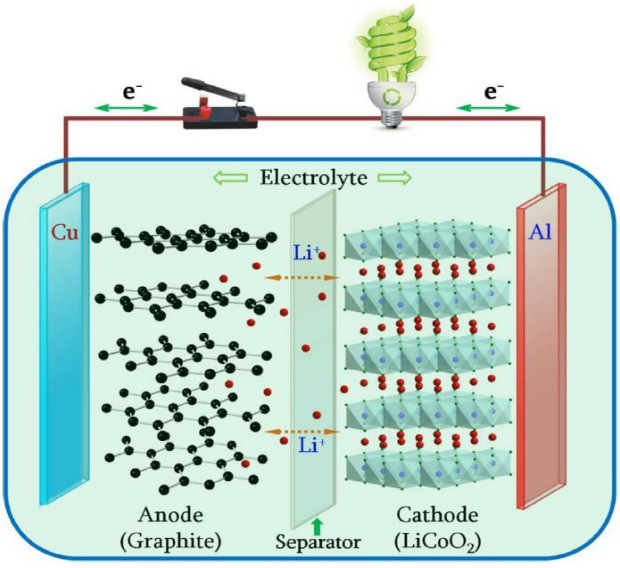

Figure 2.2 – Working mechanism of a LIB (Source: [2])

When a LIB is overcharged, it can result in battery destruction because active cathode material is saturated. The chemical reaction of this phenomenon is shown below [2].

$$LiCoO_2 + Li^+ + e^- \rightarrow Li_2O + CoO$$

The release and arrangement of charged particles into electrode structure depend on charging and discharging voltage. Therefore, charging and discharging voltage impact considerably on LIB capacity and charging time. Charging at low rate results in high capacity but requires long charging time while high charging rate shortens charging time but reduces battery capacity. Charge-discharge curves of a LFP battery at different C-rate in Figure 2.3 schematically illustrate for this principle. Furthermore, charging a battery at higher cut-off voltage can decrease cycle life and safety of this battery because it cause instability of cathode crystal structure as well as above side reaction for cathode and electrolyte solution [26].

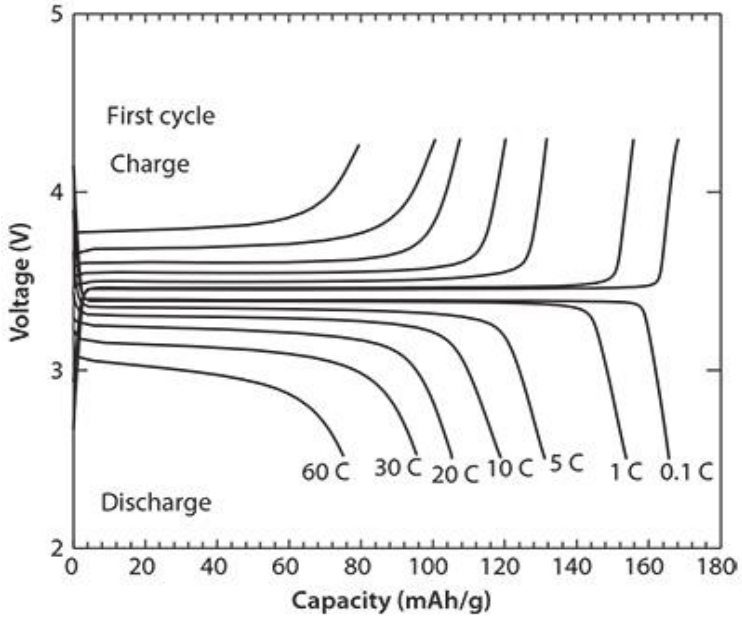

Figure 2.3 – Charge-discharge curves of LFP battery at various C-rate (Source: [27])

2.1.4 Lithium-ion battery market trends

Due to wide application, LIB market is expanding rapidly. In next decade, since electric vehicles as well as power storage systems are widely used, LIB market would significantly increase and is predicted to reach approximately 80 billion U$ in 2025 (Figure 1.1) and have 390 GWh of total electricity demand in 2030. As shown in Table 2.3, in next decade, road transportation sector will surpass portable electronics sector and become the biggest sector of LIB market when EVs, HEVs and PHEVs are progressed and proliferated. Moreover,

needs to store energy from renewable energy sources or in off-grid energy system would contribute to huge LIB demand.

Table 2.3 – LIBs applications and market (Source: [1])

	2010	2015	2020	2025	2030
Cell phones	6	11	17	28	44
Tablets	1	7	12	17	25
PC	12	9	9	9	11
Portable electronics, other	3	4	7	12	20
Portable electronics, total	**21**	**31**	**45**	**66**	**100**
EV	0	11	65	115	200
PHEV	0	2	8	13	25
HEV	0	0	2	7	15
Road-transport, other	0	0	1	2	5
Road-transport, total	**0**	**13**	**76**	**137**	**245**
Storage in power supply	**0**	**0**	**2**	**10**	**30**
Other applications	**1**	**1**	**2**	**7**	**15**
Total	**22**	**45**	**125**	**220**	**390**

2.2 Recycling methodology

A spent lithium-ion battery contains essentially valuable metallic components such as nickel, cobalt, lithium and low recovery value elements (e.g. phosphorous, Al, Fe) [6]. The recycling of spent LIBs, driven by environmental concerns and economic interests as discussed above, primarily focus on recovering highly valuable metals – lithium and cobalt in active cathode materials.

2.2.1 Spent lithium-ion battery recycling

Hydrometallurgy and pyrometallurgy or combination of them are major methods for recycling spent LIBs at industrial and research scale [6]. A typical recycling scheme, which is schematically demonstrated in Figure 2.4, commonly comprises of four major steps – Pre-treatment, metal extraction, product recovery, and production preparation.

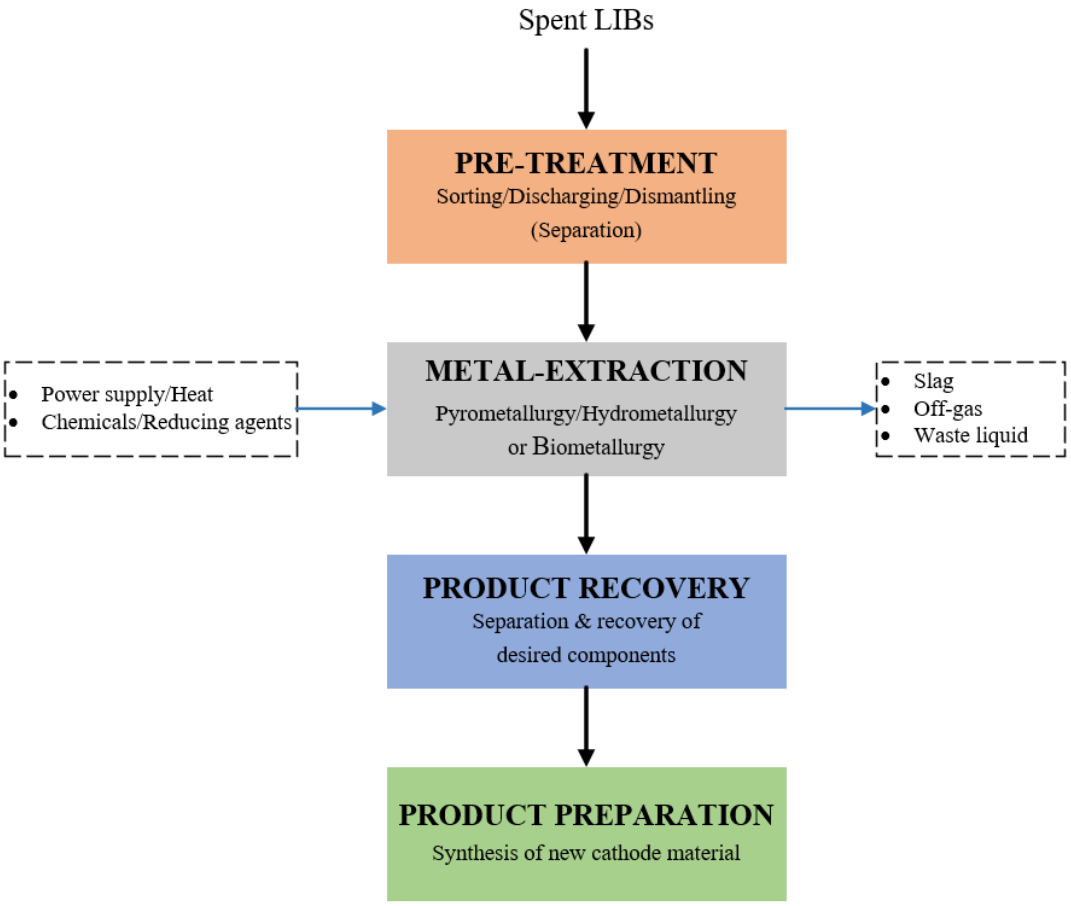

Figure 2.4 – Recycling scheme for spent LIBs (Source: [6])

2.2.1.1 Pre-treatment

Spent LIBs are, first, fully discharged to avoid any spontaneous combustion or short circuiting during subsequent dismantling step. Spent LIBs are commonly immersed in a salt solution as a method to discharge [6]. Subsequently, the fully discharged spent LIBs are processed by mechanical separation or namely, manual dismantling. This step purpose is to detach plastic casings and separate internal component of spent LIBs (e.g. cathode, anode, separator) for further recycling treatment. Then, chemical/thermal/physical treatment (e.g. scraping manually, solvent dissolution method, thermal treatment method, sodium hydroxide dissolution method, ultrasonic-assisted separation or mechanical method) is used to separate active cathode material from aluminium foil for further processing [6].

2.2.1.2 Metal extraction

Metal extraction step plays a significantly important role of the whole recycling process. In this step, metallic components in active cathode material are converted to alloy or metal ion

state, which facilitates separation and recovery of these components. The major approaches selected for this step are pyrometallurgy, hydrometallurgy, and biometallurgy.

- **Pyrometallurgy**: In this method, smelting reduction at high temperature occurs. The valuable metallic components are reduced and then recovered in alloy form [28];
- **Hydrometallurgy**: Recycling metals hydrometallurgically involves chemical leaching, which extract valuable metals from spent LIBs cathode material to solution in ion form by leaching agents. Common leaching agents employed in leaching step are ammonia-ammonium salt systems, organic acids (e.g. citric acid, oxalic acid, ascorbic acid) or inorganic acids (e.g. HNO_3, HCl, H_2SO_4) [6];
- **Biometallurgy**: This process is based organic and inorganic acid leaching created by microbial activities to extract valuable metal from spent LIBs cathode material [6, 29].

Pyrometallurgical recycling of valuable metals from spent lithium-ion batteries is simple, however, it is not eco-friendly because of its high energy usage, metal-loss rate and secondary pollution sources (e.g. waste gas, dust) [6, 30]. Biometallurgy requires low energy consumption, simple equipment, mild process conditions but slow kinetics, difficulties of cultivating bacteria and low pulp density are still major drawbacks preventing wide utilisation of this method [29]. Hydrometallurgy are commonly method applied in metal recycling due to its low energy consumption, high product purity and metal recovery rate as well. Nonetheless, the major disadvantage of this method is high chemical consumption [31]. Overall, for spent LIBs recycling, the most important priorities are economic benefits of recovered metals and their technical performance, which are crucially affected by purity of recycled metals. Therefore, hydrometallurgical approach by acid leaching is a promising method to recycle valuable metals effectively from cathode materials.

Literature investigation shows that recycling processes for spent LIBs primarily target at valuable components of cathode material (e.g. lithium, cobalt, nickel or manganese). At research scale, major methodology for metal extraction is hydrometallurgy through acid leaching of cathode material. Inorganic acids such as sulphuric acid, nitric acid and hydrochloric acid are prioritized in spent LIB recycling research because of their low price as well as high leaching efficiency while popular organic acids for leaching are tartaric acid, citric acid and oxalic acid. In addition, in order to enhance leaching efficiency without increasing acid concentration, reducing agents (e.g. Hydrogen peroxide, sodium

metabisulfite, etc.) are added to support dissolution of desired metallic components by reducing them to more soluble oxidised states (reducing Co^{3+} state to more soluble Co^{2+} state) [11]. Leaching experiments are also conducted at high temperature (from at least 50 ^{o}C) and long leaching period (at least 1 hour) to enhance collision frequency of leaching reaction (Refer to Table 2.4 and Table 2.5 for details).

2.2.1.3 Product recovery

After metal extraction step, the resulting products commonly includes many different metal ions (e.g. Li, Co, Ni). Therefore, product recovery step is required to separate and recover these valuable metals successfully. The widely used separation techniques are chemical precipitation (or selective precipitation) and/or solvent extraction [6]. Hence, the products from pyrometallurgical method require acid dissolution while hydrometallurgical or biometallurgical products are essentially leachate. Chemical precipitation or selective precipitation is a chemical technique that uses a specific reagent that can precipitate particular metallic ions while leaving other impurities or undesired substances in the aqueous solution while solvent extraction or liquid-liquid extraction is a technique to separate metallic compounds based on the difference of their relative solubilities in two immiscible liquids [32]. There are many research and report in terms of spent LIB recycling by using one of these techniques or a combination of them to recover Li, Co or Ni with promising efficiency.

Metallic components in leachate after metal extraction are researched for selective precipitation by adjusting pH of leachate and using of various precipitants (e.g. NaOH, NH_4OH, Na_2CO_3) but NaOH is still the most common precipitant while solvent extraction is also studied with different organic solvent systems (e.g. PC-88A, Cyanex 272, saponified P507, etc.). At least 90% of leaching efficiency as well as 85% of overall recovery efficiency of desired metals were reached. In addition, summaries of research for hydrometallurgical recycling of spent LIBs by selective precipitation and solvent extraction for leachate are presented in Table 2.4 and Table 2.5, respectively.

2.2.1.4 Product preparation

Main purpose of this step is purifying and prepare recovered products for further actions (e.g. synthesis of new active cathode materials, commercial sales as construction materials, etc.). Products achieved from product recovery steps are then be purified, crystallized, dewatered and oxidised to form stable solid state. They are then classified for different

purposes. Valuable components can be used for synthesis of new active cathode materials (e.g. lithium, nickel, manganese or cobalt) or commercial sales (e.g. lithium, cobalt). Others can be sold as construction materials or for steel industry.

2.2.2 Summary of spent LIBs recycling research

As discussed above, hydrometallurgical recycling is preferred because of its low gas emission as well as low energy consumption and importantly, excellent recovery rate and high product purity. These advantages, hence, overweigh its disadvantage in terms of high chemical usage and can also guarantee for good economic return of recycling process.

Additionally, leachate from acid leaching contains a variety of metallic ions. This necessitates separation of these metallic ions to recover and then produce new cathode materials or for commercial sales. Therefore, as aforementioned above, chemical precipitation and/or solvent extraction are applied. Both of them provide excellent separation efficiency as well as product purity [6].

From summaries of research results (Table 2.4 and Table 2.5), these following findings are identified as initial backgrounds for the direction of experimental works in this thesis.

- For acid leaching step, the variation of acid concentration, reductants and their concentration, pulp density (ratio of leaching liquid and solid), reaction time and especially temperature can impact directly on leaching efficiency of metals from cathodic materials of spent LIBs. Therefore, attempts for optimization of leaching stage are necessary to achieve an optimal extracting efficiency for cathodic metals with low intensity of chemical, energy and time usage.
- For product recovery step, solvent extraction and selective precipitation are both used. Solvent extraction requires usage of toxic organic chemicals as well as complicated experiment procedure, hence, selective precipitation technique, which is simpler and use less treated-intensive bases (e.g. NaOH, Na_2CO_3), is studied to, firstly, evaluate its feasibility and efficiency for metal recovery and secondly, to further aim at a process that could be easily to scale up from laboratory scale to pilot and then industrial scale.

Table 2.4 – Leaching systems for recycling spent LIBs

Recycling source	Leaching system	Time (hours)	Temp. (ºC)	Leaching efficiency (%)		Ref.
				Li	Co	
Inorganic acid leaching						
Spent LIBs (LCO)	4 mol/L HCl	1	80	99.0	99.0	[33, 34]
Spent LIBs (LCO)	2 mol/L HNO_3	2	80	95.0	97.0	[35]
Spent LIBs (LCO)	1 mol/L HNO_3 + 1.7 vol% H_2O_2	2	75	95.0	95.0	[36, 37]
Spent LIBs (LCO)	1 mol/L HNO_3 + 1.0 vol% H_2O_2	1	80	93.0	91.0	[38]
Spent LIBs (LCO)	2 mol/L H_2SO_4	1	80	~99.0	~99.0	[39]
Spent LIBs (Mixed)	1.34 mol/L H_2SO_4 + 0.45 g/g $Na_2S_2O_5$	1	20	-	96	[40]
Spent LIBs (LCO)	3 mol/L H_2SO_4 + 0.25M $Na_2S_2O_3$	3	90	99	98	[41]
Spent LIBs (LCO)	2 mol/L H_2SO_4 + 2 vol% H_2O_2	2	60	94.0	92.0	[42]
Spent LIBs (LCO)	2 mol/L H_2SO_4 + 5 vol% H_2O_2	1	75	94.0	93.0	[43]
Spent LIBs (LCO)	2 mol/L H_2SO_4 + 6 vol% H_2O_2	1	60	97.0	98.0	[44]
Organic acid leaching						
Spent LIBs (LCO)	1.25 mol/L $C_6H_8O_6$	0.33	70	99	95	[45]
Spent LIBs (NCM)	0.5 mol/L $C_6H_8O_7$ + 1.5 %vol. H_2O_2	1	90	98.1	98.8	[46]
Spent LIBs (LCO)	1mol/L $H_2C_2O_4.2H_2O$	2	80	98.0	98.0	[47]
Spent LIBs (NMC)	3 mol/L TCA + 4 vol% H2O2	0.5	60	100	96	[11]
Spent LIBs (LCO)	2 mol/L $C_4H_6O_6$ + 4 %vol. H_2O_2	0.5	70	99.1	98.6	[48]
Spent LIBs (LCO)	0.4 mol/L $C_4H_6O_6$+0.02 mol/L $C_6H_8O_6$	1	80	95.0	93.0	[49]
Spent LIBs (LCO)	0.5 mol/L glycine +0.02 mol/L $C_6H_8O_6$	2	80	-	91.0	[50]

Table 2.5 – Research for metal recovery from spent LIB leachate

Reagents	Efficiency (%)		Ref.
	Li	Co	
Solvent extraction			
0.9 mol/L P507 (or PC88A)	100.0	80.0	[34]
1 mol/L Cyanex 272 + 10 wt% Acorga M5640	-	> 97	[51]
1.5 mol/L Cyanex 272	-	85.4	[52]
50% saponified 0.4 mol/L Cyanex 272	1	95-98	[44]
25% of 70% saponified P507	8	65	[45]
7 % PC88A + 2 %AcorgaM5640 + Cyanex 272	-	90	[53]
10 vol% PC88A + 5 vol% TOA	-	98	[54]

Selective precipitation			
NH_4OH/NH_3 (reverse precipitation) at pH = 11 and 25 ^oC	-	92	[55]
2 mol/L NaOH at pH = 0.5 and room temperature	-	44	[56]
4 mol/L NaOH at room temperature and pH = 6-8	-	> 90	[57]
5 mol/L NaOH at pH = 5 and room temperature	-	97.8	[58]
10 mol/L NaOH at pH = 10 and room temperature	> 99	-	[35]
40% NaOH at pH = 4.6-6.0	-	> 89	[59]
NH_4OH/NH_3 at pH ≥ 6 and 50 ^oC	> 40	> 60	[60]
$(NH_4)_2C_2O_4$ + Na_2CO_3 at pH =2-2.5 and 50 ^oC	71.0	94.7	[42]
2.0 mol/L NaOH + Saturated Na_2CO_3 + Saturated NaOH at pH = 9 and 11-12 and at room temperature	90	95	[61]
Mextral 272P and 0.5 mol/L Na_3PO_4 at room temperature and pH > 8	95.8	97.8	[62]

2.2.3 Industrial recycling process for LIBs

Industrial processes for recycling spent battery are commonly combinations of hydrometallurgical and/or pyrometallurgical and/or mechanical unit operations [10]. In this sections, well-known hydrometallurgical and pyrometallurgical recycling processes are briefly introduced including of Umicore, Toxco and Inmetco processes.

2.2.3.1 Umicore process

This battery recycling process is one of the most common industrial recycling processes for spent LIBs and NiMH batteries. Umicore process is the integration of hydrometallurgical and pyrometallurgical unit operations without any pre-treatment for spent batteries. This process target is to primarily recover Ni, Co and Cu as alloy. Lithium and rare earth elements are recycled from slag fraction of process. The simple flow sheet describing Umicore recycling process is shown in Figure 2.5.

In this process, the Isa Smelt furnace technology is applied to reduce mechanical pre-treatment for spent batteries. When the furnace is in operation, it has three different temperature zones:

- **The top pre-heating zone**: temperature is kept below 300 ^oC in this zone to evaporate the battery electrolytes. The slow heating minimises the explosion risks of dangerous chemicals in electrolytes [63];

- **The middle pyrolysing zone**: This zone is to remove plastics of spent battery with a maintained temperature of approximately 700 ^{o}C. In addition, this exothermic removing process provides the energy to the top zone [63];
- **The bottom smelting zone**: This zone with temperature around 1,200-1,450 ^{o}C is to separate the remaining battery components into alloy phase and slag. Cobalt, copper, nickel and irons constitute alloy phase whilst the slag includes lithium oxides and some other metal oxides. The alloy undergo further hydrometallurgical treatments and the separated slag is sold as construction materials [63].

Nickel, cobalt, zinc, copper and iron are then dissolved and precipitated to recover from alloy phase. Nickel and cobalt are recovered in the form of nickel hydroxide ($Ni(OH)_2$) and cobalt chloride ($CoCl_2$), respectively. The cobalt chloride then can be oxidised and burnt with $LiCO_3$ to produce new cathode material – lithium cobalt oxide (LCO) [10]. No mechanical pretreatments for spent batteries and good recovery rate for valuable metallic components (e.g. cobalt, nickel) are major advantages of this process [18].

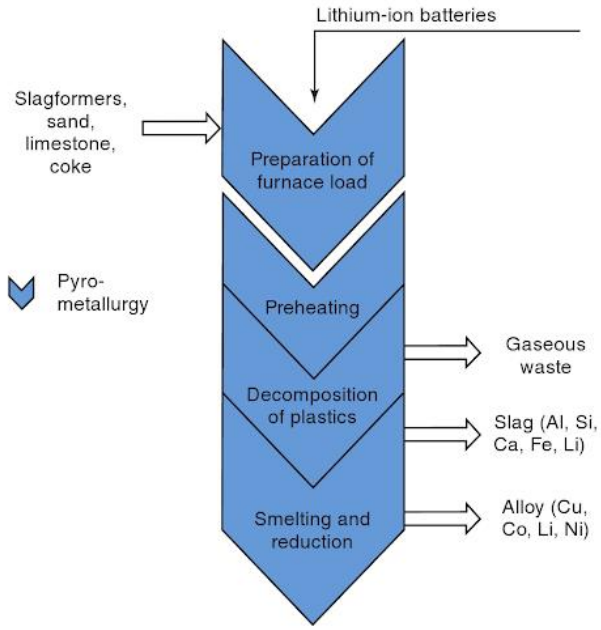

Figure 2.5 – Umicore recycling process flowchart (Source: [64])

2.2.3.2 Toxco process

The Toxco process is based on hydrometallurgy method to recycle spent LIBs. This process includes battery pre-treatment, component separations, leaching, purification of solution and lithium precipitation [63]. The Toxco process flow sheet is shown in Figure 2.6.

In patented pre-treatment with cryogenic cooling, spent batteries are cooled down to around -175÷-195 ^{o}C by liquid nitrogen [63]. This range of temperature sufficiently reduce the reactivity of battery components below explosion thresholds. In addition, this cryogenic temperature makes the plastic casing of spent LIBs brittle, hence they are easily broken. The refrigerated batteries are then shredded and put through hammer mill to grind the batteries in a lithium brine. The lithium component dissolves during hammer milling to form a solution of $LiSO_3$, LiCl, Li_2CO_3. The lithium solution and undissolved products are separated by the screw press equipped in the hammer mill. The undissolved products are so-called fluff and the lithium solution requires more treatments due to undissolved components including fine carbon and metal oxide. The fluff is then put through a shaking table to separate low density mixture of stainless steel and plastics from high density cobalt-copper mixture. These products are all packed and sold. The lithium solution is stored in a holding tank before filtration. The solution pH is adjusted by using lithium hydroxide instead of sodium hydroxide to avoid contamination of sodium in lithium product. The solution in holding tank undergoes dewatering, filter pressing and purification process to form final product Li_2CO_3.

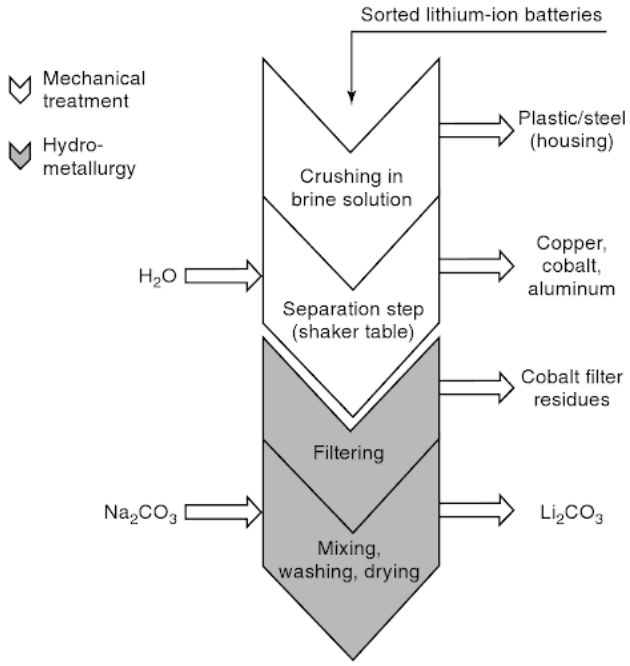

Figure 2.6 – Flowchart of Toxco process for recycling spent LIBs (Source:[64])

2.2.3.3 INMETCO Process

The International Metals Reclamation Company (INMETCO) process applies pyrometallurgical method for treating metallic waste comprising spent batteries. The process entails (1) feedstock preparation, mixing and pelletising; (2) component reduction; (3) melting and alloy casting [65]. Figure 2.7 schematically depicts the INMETCO process.

The end-of-life batteries are first dismantled, removed plastic casing, drained their electrolytes and shredded. The other type of solid waste is mixed with a carbon reductant [63]. The solid mixture is then turned to pelletised form with nickel and cadmium liquid waste addition during pelletising step. These pellets are subsequently mixed with shredded spent batteries before introducing to reduction stage.

Reduction stage is conducted at 1260 ºC with 20 minute residence time to reduce metal oxides to metals [63]. The off-gas of this step is scrubbed and the scrubbing liquid is fed to wastewater treatment facility before treated water is circulated to the process. The reduced mixture undergoes smelting stage to create an alloy including nickel, iron, chromium and manganese. The alloy is casted to form pig alloy and then are consumed by stainless steel industry.

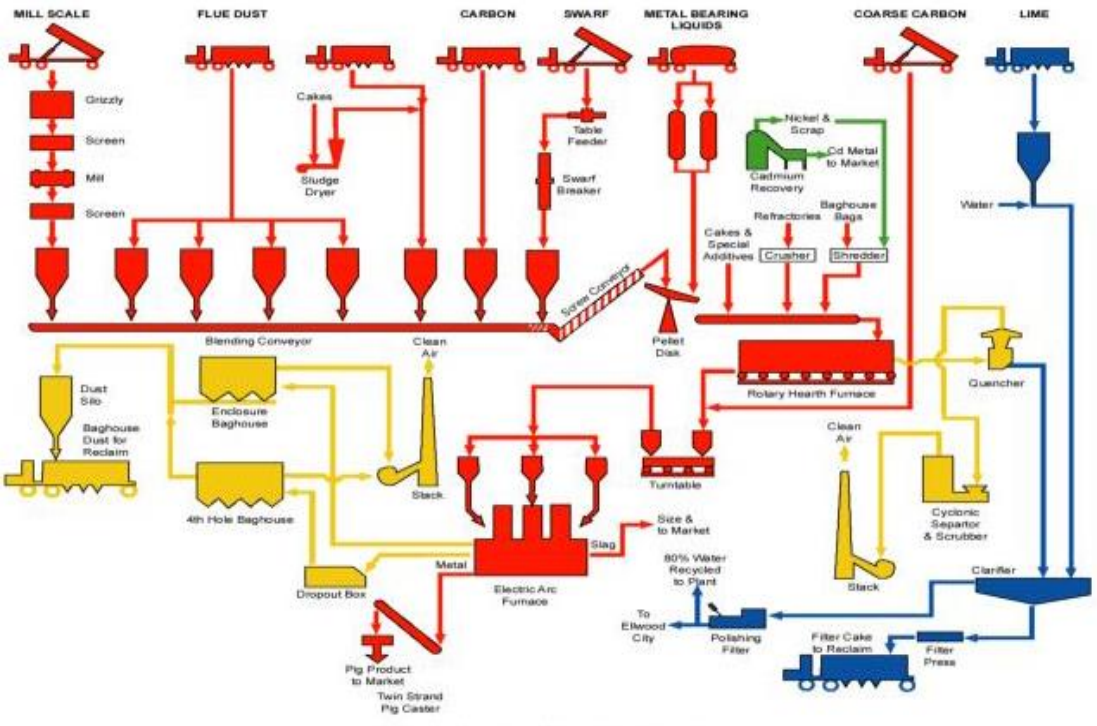

Figure 2.7 – Flow diagram of INMETCO process (Source: [65])

Overall, these processes and recycling facilities as well as governmental stringent regulations for recycling (e.g. China, Europe) are demonstrating our significant attempts to process this special type of waste (spent LIBs). However, as mentioned above, only approximately 5% of spent LIBs are currently recycled [7], this means current processes for recycling are not sufficient to handle disposed LIBs amount. In addition, these current processes can only recover moderate proportion of alloy metals in spent LIBs (e.g. Co, Ni, Cu). The final slag, which is sold with low prices as construction materials, still contains high amount of unrecovered valuable components (e.g. Co, Li, Ni, etc.). It results in less economic attraction of current recycling processes while they require high energy consumption as well as collection and transportation cost [6]. Enhancing quality of recycled products (i.e. recycling effectively and purely valuable components) from spent LIBs can increase profit and attract more investment for the recycling of this waste. This could lead to sufficiency of recycling facilities for enormous quantity of spent LIBs. Hence, the development of effective and efficient recycling scheme for recovering high value metals from spent LIBs is the key in improving global sustainability.

2.3 Analytical techniques in project

SEM-EDS, AAS and XRD were used in this project for qualitative and quantitative analysis for both solid and liquid samples. The basic mechanisms of each technique are covered in this section as mentioned at the beginning of the Literature Review.

2.3.1 Scanning Electron Microscopy / Energy Dispersive X-Ray Spectroscopy (SEM-EDS)

The Scanning Electron Microscopy / Energy Dispersive X-Ray Spectroscopy (SEM-EDS) is a non-destructive analytical technique to evaluate or analyse testing sample. This analytical technique is developed to overcome the current limitation of analytical techniques that electron beams are commonly reflected or absorbed in the sample rather than passing through the sample [66].

Physically, electron beams (primary electrons) are not only merely backscattered but also can provide atomic electron energy for examined sample and then released as secondary electrons. Based on this mechanism, in SEM analysis, focused electron beams with high energy are magnified and directed by electron lenses to hit samples in a vacuum chamber and the topography images of specimen surface are form based on detected secondary

electrons. Two widely used detectors in SEM are the Backscattered Electron (BSE) Detector and the Secondary Electron Detector (SED) [67].

Energy Dispersive Spectroscopy (EDS) analysis is commonly utilized simultaneously with SEM to analyse the element composition of specimen surface. Similar to SEM, EDS is also based on unique energy of X-ray beam reflection from specimen reflections, which are relatively specific to different chemical elements [66]. In the vacuum chamber for testing, the X-rays reflected from inspected specimen are then detected by EDS detector and then interpreted to elemental information of specimen [67].

Generally, SEM presents the visual information while EDS supplies the chemical concentration of inspected specimen. These techniques are commonly used simultaneously and referred as SEM-EDS analysis. The main limitation of this analysis is the reliance on type of window for light element detection because common Beryllium window only allows for element detection typically above atomic number of sodium. For lighter elements, polymer-based windows are required with appropriate operating conditions [68].

2.3.2 Atomic Absorption Spectroscopy (AAS)

Atomic Absorption Spectroscopy (AAS) is a quantitative measurement of chemical elements in testing liquid sample. Essentially, different element atoms absorb distinct light wavelength due to characteristic arrangement of outer shell electrons. Therefore, the radiation (e.g. ultraviolet or visible light) is utilized to excite the sample atoms, which have promotions to higher energy level through energy absorption from photon radiation. This absorbed energy amount is distinctive to a specific electron promote of a particular element [69].

Basically, the inspected sample is firstly vaporised and atomised to convert atoms to their ground state in the vapour phase. Subsequently, electromagnetic radiation released from radiation source (e.g. Hollow Cathode Lamp – HCL, Electrodeless Discharge Lamp – EDL) is passed through the atomised sample [70]. A detector is utilized to measure and compare the light wavelengths transmitted from inspected sample with the initial wavelength of radiation from radiation source [70]. The variations of wavelength are then processed and compared with calibration curves by a signal processor to provide an element concentration in the inspected sample. The calibration curves of target elements are constructed beforehand by analysing known concentration samples of target elements under the same testing conditions of the inspected sample [69].

The AAS analysis allows the measurement down to parts per billion of a gram of inspected sample [69]. In addition, this technique is widely used to identify the concentration of specific metallic elements in a sample and can determine more than 62 different metal concentrations in an inspected solution with high precision, especially lower waiting time and cost than ICP-OES (Inductively Coupled Plasma – Optical Emission Spectroscopy) or ICP-MS (Inductively Coupled Plasma Mass Spectrometry) [70].

2.3.3 X-ray Powder Diffraction (XRD)

The X-ray Powder Diffraction (XRD) is an analytical technique that uses X-ray diffraction for phase identification as well as crystalline properties of crystalline samples. This technique is widely used for determination of unknown crystalline samples, which is critical for studies and research in engineering, material science, geology or biology.

Any crystalline phase has its own periodic atomic or molecular packing of unit cell. The 3D periodic arrangement of unit cell can form various groups of lattice planes [71]. When incident X-ray beams interfere with lattice plane in analysed sample, it results in a specific X-ray diffraction pattern of this lattice plane. Each X-ray diffraction pattern is unique and only characteristic for a specific substance. Therefore, the X-ray diffraction pattern from sample is collected and compared to standard patterns of different substances to determine what the analysed sample is.

In XRD analysis, the X-ray beams are generated from a cathode ray tube. This tube includes a filament, which is heated to produce electron beams. These beams are then accelerated by a voltage and targeted to analysed sample. The interaction of incident X-rays with electron shell of analysed sample results in the characteristic X-ray diffraction. The X-ray diffraction in XRD analysis is based on Bragg's law [71]. A detector is used to record and process diffracted X-ray signal into a count rate (intensity). During XRD analysis, the incident beam and detector are rotated in a circle around the sample (i.e. in XRD system, the analysed sample is rotated instead of incident beam and detector to simplify XRD equipment) [72]. The detector records the X-ray intensity at each rotated angle (2θ). The intensity of diffracted X-rays at different rotated angles are records and form the X-ray diffraction pattern of analysed sample. because it directly relates to crystal structure. This pattern, as mentioned above, is compared to standard patterns to identify unknown substance in analysed sample.

This technique is a very powerful qualitative analysis to determine unknown powder materials, their composition and crystalline characterizations, identification dimensions of unit cell, rough measurement of purity [71]. However, it requires homogeneous and single-phase sample for optimal analysis result and can only provide approximately 2% detection limit of sample [71].

3 EXPERIMENTAL

3.1 Materials and chemicals

Raw materials and chemicals used for experiments in this thesis are

- Lithium cobalt oxide (LCO) powder from spent iPhone batteries;
- Commercial LCO powder;
- 98 wt% sulphuric acid as acid medium for leaching;
- Sodium metabisulphite ($Na_2S_2O_5$) with 97% purity and 30 wt% hydro peroxide (H_2O_2) as reducing agent;
- 2 wt% nitric acid for stabilizing and diluting samples;
- NaOH 1M and Na_2CO_3 1M for selective precipitation.

3.2 Pre-treatment

Spent iPhone batteries are chosen due to their abundant quantity and ease of supply connection. To prevent short circuiting, battery voltage was first measured by a voltmeter to test remaining capacity of spent batteries. Normal LIB voltage is commonly 3.4-4.1 V [10]. Hence, for safe dismantling, a lower measured voltage than this range is required.

To minimize possible explosion as well as toxic electrolyte risks, spent LIBs were carefully dismantled in a fume hood. A plastic cutting knife was used to remove plastic outer casing of LIB. Enveloping polymer film and aluminium cathode collector layer were then dismantled. iPhone 6 battery disassembly is shown in Figure 4.1. Cathode and anode stacked layers were then uncovered, separated from each other and then unfolded. Manual scrapping was then executed to achieve active cathode material – LCO. Component and morphology of solid material was then identified by AAS and SEM-EDS analysis respectively.

3.3 Acid leaching

Since this thesis aims at recovering high quantity of lithium and cobalt from spent active cathode material. Therefore, acid leaching plays a significantly important role for overall

recover efficiency. In this step, metallic components are dissolved as ions in acid environment. Optimal acid leaching can enhance efficiency of subsequent metal separation step. Therefore, optimization of acid leaching is necessary to identify appropriate conditions for highest efficiency of acid leaching without waste of chemical or energy.

Leaching step in this thesis was conducted in sulphuric acid medium. Because in previous work of this recycling project, H_2SO_4 provided higher leaching efficiency than HCl and HNO_3 [73]. Acid concentration, leaching temperature as well as leaching time are important contributing factors to high leaching efficiency [42]. In addition, presence of reducing agents is necessary to reduce insoluble Co^{3+} state in LCO to soluble Co^{2+} state, hence, it decreases required acid quantity and avoid risks of handling with high concentrated acid [74, 75]. In this thesis, sodium metabisulphite ($Na_2S_2O_5$) and hydro peroxide (H_2O_2) are investigated. The former is the most effective reducing agent based on previous work of this project [73] while the latter is emerging as an new promising reducing agent in recent recycling research. Moreover, pulp density (i.e. ratio of LCO powder to leaching liquid) is also an important factor contributing to leaching efficiency of metals [76]. Experiments for leaching condition investigation were conducted in 100 mL glass beaker on a stirring hot plate. Influences of the following factor alteration are researched

- Acid concentration (at 1.0, 2.0, 3.0 and 4.0 M),
- Reducing agents ($Na_2S_2O_5$ and H_2O_2),
- Reducing agent concentration (at 1, 2, 3, 4 wt%),
- Leaching time (leaching in 2, 4, 6 and 8 hours),
- Leaching temperature (at 25, 40, 60 and 80 ^oC) and
- Pulp density (at 10, 13.3, 20, 30 and 40 g/L).

As varying one factor, others were kept constantly at 40 ^oC, 2 hours for leaching, 2 mol/L H_2SO_4, 20 g/L pulp density, 2 wt% H_2O_2 as reducing agent. The optimal value of each factor has to provide optimal leaching efficiency of lithium and cobalt with lowest energy and time consumption. Refer to Figure 3.1 for experiment setup for acid leaching and vacuum filtration. Resulting mixture after leaching was then liquid-solid separation by vacuum filtration. Liquid phase was then diluted with 2 wt% nitric acid for stabilization. These diluted liquid samples were then AAS analysed for leaching efficiency of cobalt and lithium.

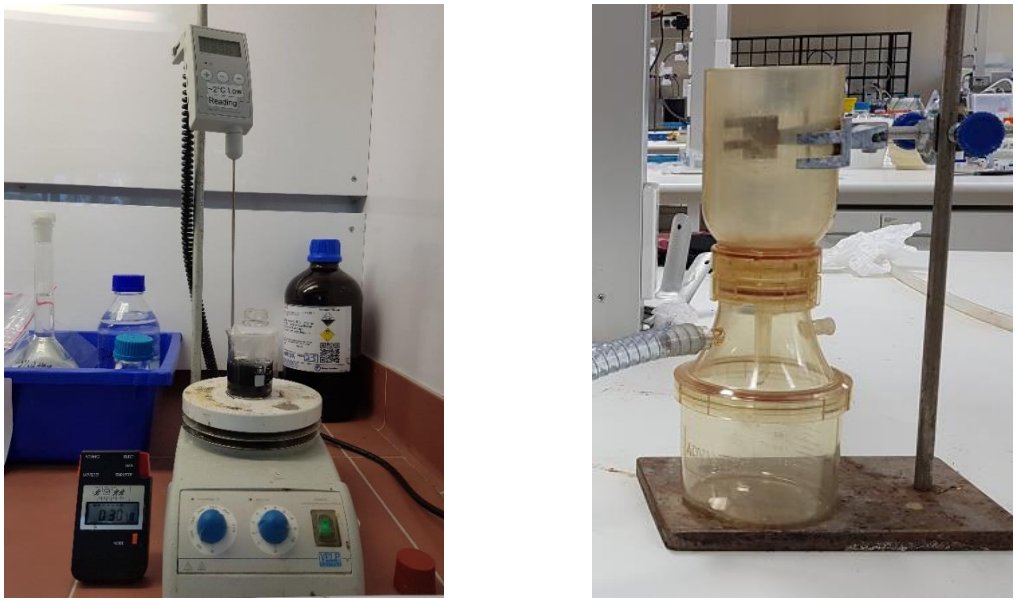

(a) **(b)**

Figure 3.1 - Experiment setups in acid leaching stage
(a) For acid leaching tests. (b) For vacuum filtration.

3.4 Selective precipitation

The leachate achieved from acid leaching of cathodic material of spent iPhone batteries has high amount of many metallic ions. Hence, there is unavoidable requirement for separating and recovering these metals in solid forms. As mentioned above, there are two major methods for this stage, which are selective precipitation and solvent extraction. Solvent extraction is a complicated technique and uses organic compounds, which requires further post-treatment steps for them. In addition, using solvent extraction would make scaling-up process more complex as well. Therefore, in this thesis, selective precipitation, which is simple and requires less post-treatment intensive chemicals (e.g. NaOH, Na_2CO_3), is studied to clarify whether solvent extraction is inevitably necessary or selective precipitation is sufficient for separating and recovering lithium and cobalt.

Theoretically, cobalt and lithium can be selectively separated from leachate as well as each other. Pourbaix diagram of cobalt (Figure 3.2 - (a)) depicts that Co^{2+} state could precipitate as hydroxides in pH range of ~10-12. When pH exceeds approximately 12.5, hydroxide precipitates redissolve in solution due to the formation of complex compounds. While lithium has no precipitation in hydroxide environment up to pH = 14 and only precipitates as Li_2CO_3 from pH = 9 to 14 (Figure 3.2 - (b)). Hence, increasing pH of leachate to 12 by NaOH addition before adding Na_2CO_3 to raise pH to 14 could theoretically separate cobalt and lithium as hydroxide and carbonate precipitates, respectively.

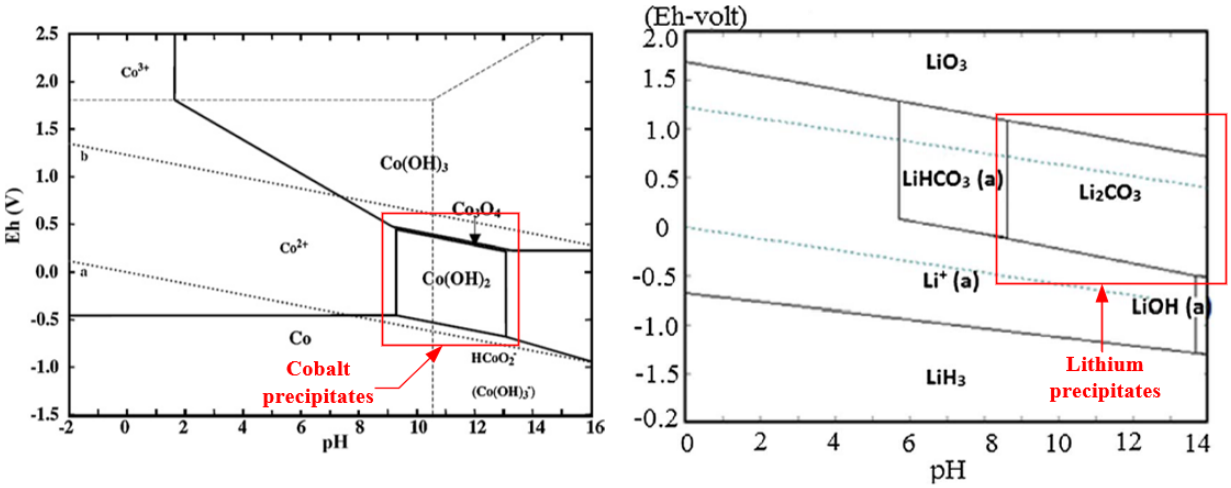

(a) **(b)**

Figure 3.2 – Pourbaix diagrams of metals in leachate at room temperature (a) cobalt-water system. (b) lithium-water system (Source: [77, 78])

Because in the leaching stage, Co^{3+} in cathodic material is reduced to Co^{2+} by adding reductants (H_2O_2 or $Na_2S_2O_5$). The achieved leachate would contain Co^{2+} state of cobalt. Hence, in this stage, to selectively separate lithium and cobalt as precipitates, NaOH 1M is added to leachate from acid leaching stage in order to increase pH to approximately 12. Hydroxide precipitates of cobalt ($Co(OH)_2$) is filtrated and then calcined to form Co_3O_4 product. Then, Na_2CO_3 is subsequently added to remaining liquid to precipitate lithium as carbonates (Li_2CO_3). Figure 3.3 - (a) schematically demonstrates experimental procedure of selective precipitation stage. In this stage, addition of NaOH stops at pH = 12 is to guarantee no formation of cobalt complex compounds. This phenomenon results in redissolution of cobalt precipitates, therefore, reducing recovery efficiency of cobalt.

Initial leachate as well as filtrated liquid after every filtration at certain pH values (2, 6, 10, 12, 13, 14) are sampled for AAS analysis to determine lithium and cobalt concentration as well as calculate recovery efficiency of each metal. During selective precipitation stage, pH of liquid is measured and controlled by WP-91 Dissolved Oxygen-pH meter (Figure 3.3 - (b)). Experimental setup for filtration is similar to setup in acid leaching stage (Figure 3.1 – (b)).

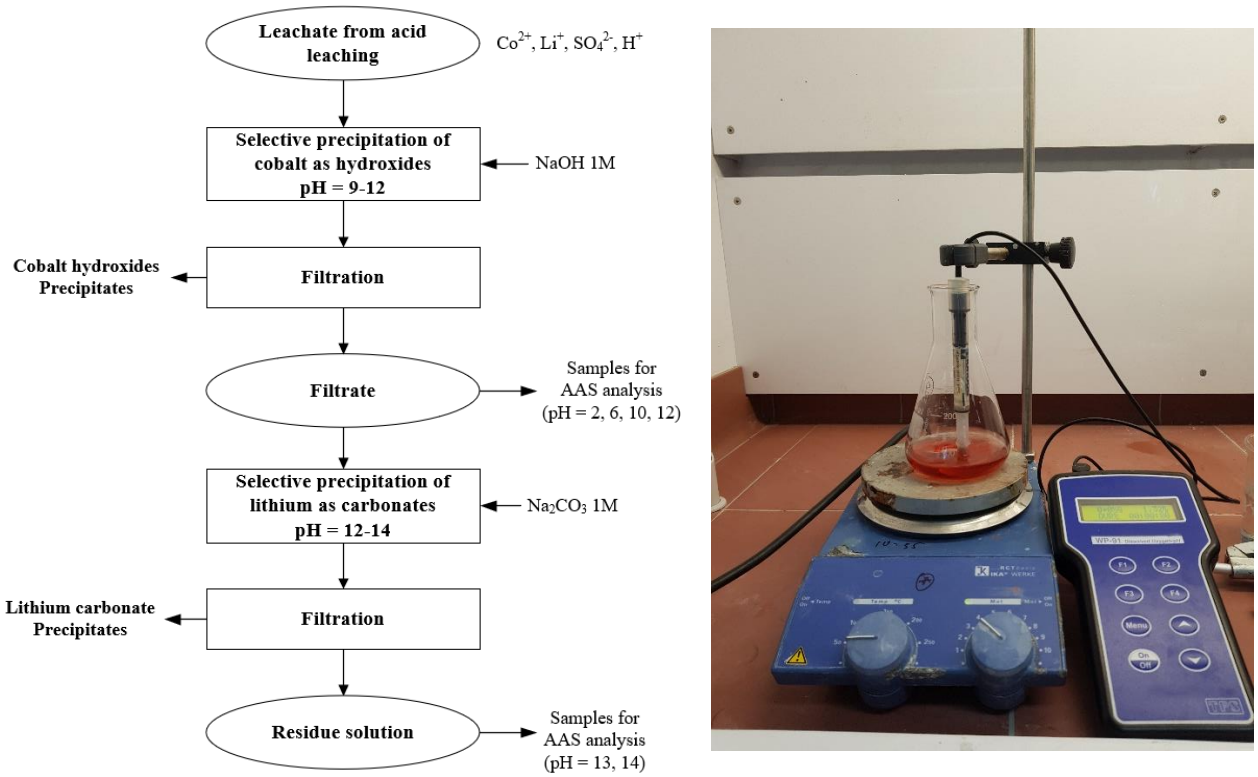

Figure 3.3 – Experimental procedure of selective precipitation stage (a) and experiment setup (b)

3.5 Cathodic material resynthesis

The recovered Li_2CO_3 and Co_3O_4 products were used as precursors for resynthesis of $LiCoO_2$. They were mixed and then calcined in laboratory oven at 600 ^oC in 24 hours for solid-state reaction to form new $LiCoO_2$ powder. The formation of $LiCoO_2$ from this solid-state reaction is as following [79].

$$2Co_3O_4(s) + 3Li_2CO_3(s) + 0.5O_2(g) \longrightarrow 6LiCoO_2(s) + 3CO_2(g) \quad (1)$$

3.6 Fabrication of new lithium-ion battery from recovered product

The achieved product from calcination is used as cathodic material in new LIB. The coin cell LIB is chosen due to its simple structure and compact size, therefore, the evaluation of electrochemical properties for recovered product can be faster as well as easier. The fabrication procedure of coin cell LIB is as following and the coin cell battery structure is schematically illustrated in Figure 3.4. The cell battery is sealed hermetically in glove box. This is to avoid the exposure of lithium-containing component to atmosphere, which can cause decomposition of them.

- The synthesized LCO (recycled cathodic product) was mixed with carbon material, binder (PVDF). The mixture was then combined with NMP solvent to form consistent slurry of cathodic material;
- The slurry was then casted onto surface of aluminium foil by the doctor blade technique. This is to form the cathode of new LIB;
- However, the cathode must be dried in oven for 6 hours at 110 ^{o}C to successfully fabricate;
- The anode was made from casting graphite on copper foil with similar procedure for constructing cathode.
- After cathode and anode were ready, the coin cell LIB was then fabricated in glove box as the procedure shown in Figure 3.4;
- The electrolyte is $LiPF_6$ in EC/DMC solvent.

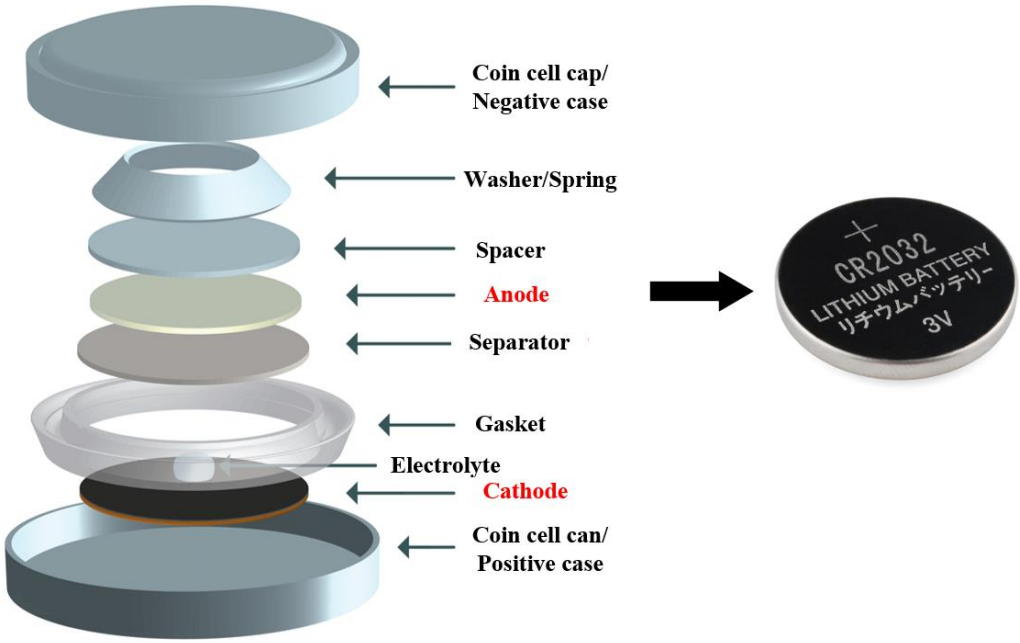

Figure 3.4 – Procedure of fabricating coin cell LIB in glove box

Besides the LIB assembled from recycled cathodic products, the commercial LCO powder is also used as cathodic material to fabricate another coin cell LIB. This is to evaluate the electrochemical performance of LIB assembled from the recycled cathodic products and the LIB fabricated from the commercial LCO powder. The electrochemical tests include the call testing by using LAND battery testing system and the impedance testing by the VSP biologic potentiostat. The LAND system is set up at a 5 mA current and a range of 3-4.2 V voltage. The impedance testing is set up at a 5 mA amplitude and a range of 0.1-100 kHz frequency.

3.7 Analytical techniques used in the project

Microstructural as well as elemental characterizations of LCO powder after dismantling as well as of selective precipitates were achieved through SEM-EDS analysis. Leachate from acid leaching as well as after selective precipitation were analysed by AAS analysis. XRD is necessary to determine what recovered precipitates are as well as their crystalline features. AAS analysis is conducted by AAnalyst^{TM} 400 system while Hitachi TM3030 SEM system is used for SEM-EDS analysis and Bruker D8 Advance powder XRD system is for XRD analysis (Figure 3.5).

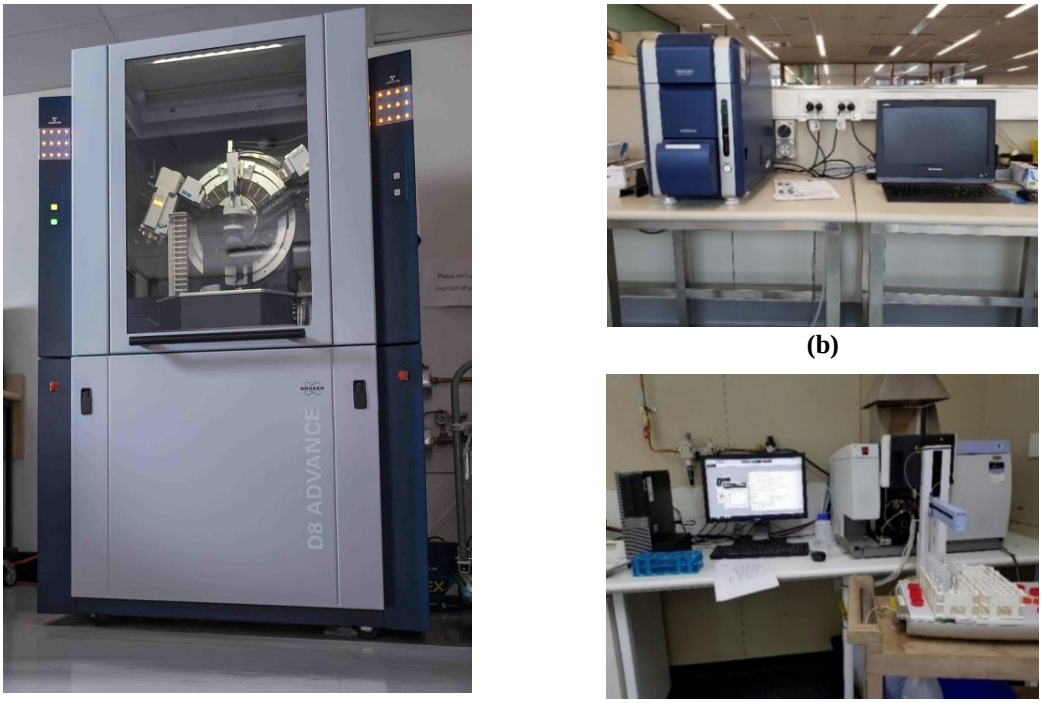

(a) **(b)** **(c)**

Figure 3.5 – Analytical systems for sample analysis
(a) Bruker D8 Advance powder XRD. (b) Hitachi TM3030 SEM system. (c) AAnalyst™ 400.

4 RESULTS AND DISCUSSION

4.1 Pre-treatment

As aforementioned, voltage measurement prior dismantling is extremely necessary to guarantee those spent batteries are dead. Hence, short circuiting and explosion risks can be eliminated. Permanent-dead voltage range of spent LIBs is commonly below 2.8-3.0 V [80]. Therefore, spent LIBs with measured voltage varying in or below this range are technically safe for dismantling. Voltage and LCO mass achieved from cathode foil of these batteries are summarised in Table 4.1. The voltage of spent LIBs in experiment are well below the

voltage range mentioned above. This means they are completely safe for dismantling. Therefore, dismantling, unpacking and unfolding component layers of spent LIBs were conducted. Figure 4.1 shows dismantling procedure for spent iPhone battery. Figure 4.2 presents unfolded component layers of an end-of-life iPhone 3 battery from multiple dismantled LIBs. The cathodic material (i.e. LCO powder) was then analysed by SEM-EDS and AAS before undergoing acid leaching for metal extraction.

Figure 4.1 – Spent iPhone battery dismantling

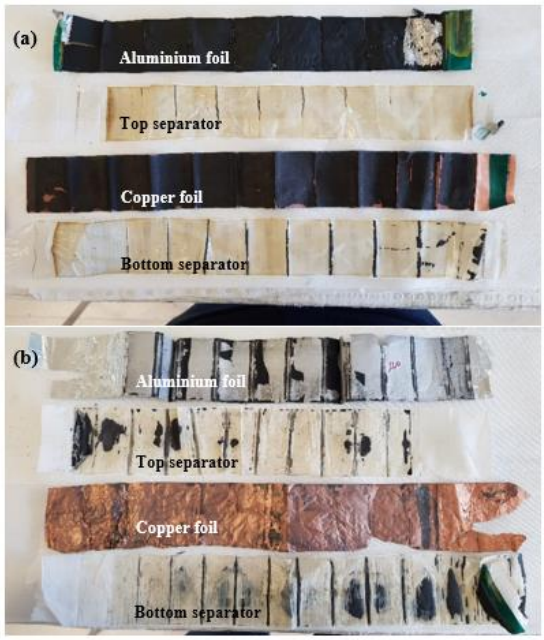

Figure 4.2 – Unpacked component layers of two iPhone 3 batteries
(a) Component layers of iP3-001 battery (Before scrapping). (b) Component layers of iP3-001 battery (After scrapping).

Table 4.1 – Specification of dismantled spent LIBs

Battery no.	Battery source	Prior dismantling voltage (V)	Cathodic material mass (g)
iP3-001	iPhone 3	1.7	4.9778
iP3-002	iPhone 3	1.8	5.0249
iP5-001	iPhone 5	1.3	4.0291
iP6-001	iPhone 6	2.0	5.2015

4.2 Initial analysis of active cathode material

Figure 4.3 shows the image of LCO powder scrapped from the spent iPhone batteries. This LCO cathodic material was then tested by SEM-EDS and AAS for qualitative and quantitative analysis.

Figure 4.3 – LCO powder achieved from spent iPhone batteries

Figure 4.4 – (a) shows SEM images of raw LCO powder at 500x magnification. Cathodic material particles have a variety of granular size. Small granular particles could result from corrosion and damages of original LCO powder due to continuous discharging and charging. During charging and discharging, fluctuation of LCO volume formed regular expansion and contraction, which gradually cause corrosion and pulverization of LCO grain. The grain degradation and battery exhaustion of spent LIBs create high grain boundaries as shown in Figure 4.4 – (a). This leads to high surface area and accessibility of LCO powder with leaching solution, which could contribute to high leaching efficiency of metals.

Figure 4.4 – (b) is a SEM-EDS image of SEM image in Figure 4.4 – (a). It provides an EDS micro-analysis that depicts the presence of elements in cathodic material. From Figure 4.4 – (b), cobalt and oxygen are major components that constitute cathodic material. The minor presence of carbon and phosphor can result from contamination or unexpected contact between anode and cathode during initial fabrication of new LIB as well as dismantling spent LIB to get cathodic materials. The lithium presence in cathodic material cannot be detected

by EDS spectra because of extremely low atomic energy of this element. Therefore, AAS analysis is used because it can quantitatively detect both lithium and cobalt. This would ensure precision of quantitative analysis for calculations of recovery efficiency.

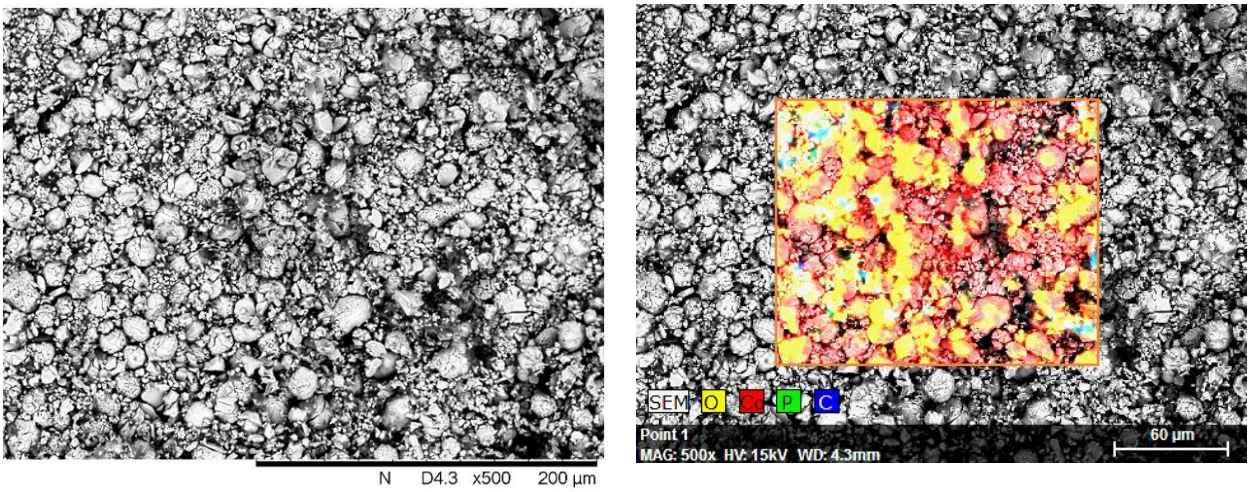

(a) **(b)**

Figure 4.4 – Cathodic material images from SEM-EDS analysis
(a) SEM image; (b) SEM-EDS analysis image

The chemical composition of raw cathodic material from spent LIB cathodes includes 8.28 wt% lithium and 65.80 wt% cobalt (Table 4.2). The cathodic material was completely dissolved and the achieved liquid was then analysed by AAS technique to guarantee accuracy of quantitative analysis. The stoichiometry ratio of lithium to cobalt is approximately 1.07, which is close to theoretical ratio in LCO – 1.1 [79]. High weight concentration of cobalt in LCO powder demonstrates serious waste if spent LIBs are just landfilled or recycled as construction materials.

Table 4.2 – Raw LCO powder composition

Element	Lithium	Cobalt
Wt%	8.28	65.80

4.3 Acid leaching of metals from active cathode material

Acid leaching experiments were conducted to optimize process parameters through investigating effect of acid concentration, reducing agent type and concentration, leaching time and temperature as well as pulp density. Therefore, dissolution of metals (i.e. lithium and cobalt), which present in cathodic LCO powder, can reach maximum. The achieved results are discussed as below.

4.3.1 Effect of acid concentration on metal leaching

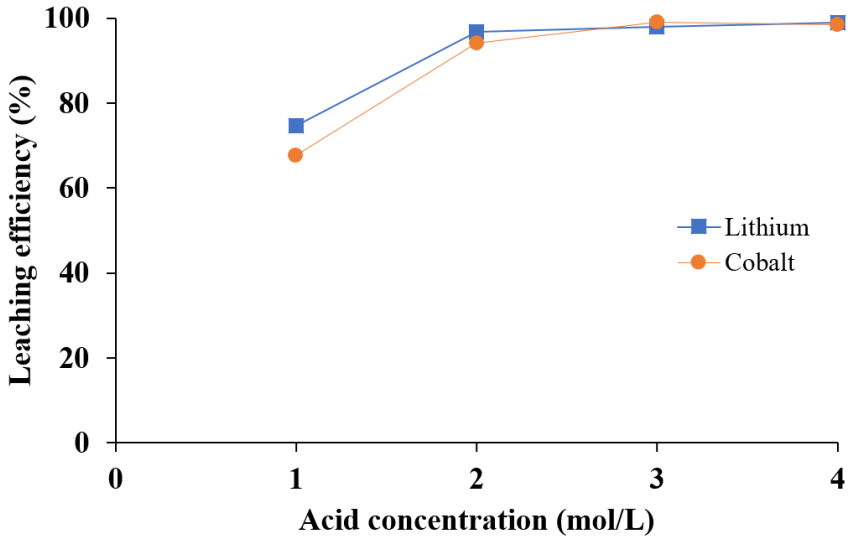

Figure 4.5 – Effect of acid concentration
[2 wt% H_2O_2; Time: 2 hours; Temperature: 40 °C; Pulp density: 20 g/L]

Sulphuric acid concentration plays an extremely important role in metal dissolution. Hence, research was conducted at different concentration varying from 1 mol/L to 4 mol/L to find optimal value. Chemical reaction between H_2SO_4 and LCO powder with the presence of H_2O_2 is shown as followed [74].

$$2LiCoO_2 + 3H_2SO_4 + 3H_2O_2 \longrightarrow 2CoSO_4 + Li_2SO_4 + 6H_2O + 2O_2 \quad (1)$$

Figure 4.5 depicts an increase of cobalt leaching from 67.62% to 98.54% as increasing sulphuric acid concentration from 1 mol/L to 4 mol/L, respectively. Simultaneously, lithium dissolution also rises from 74.61% to 98.89% with similar increase of acid concentration. Since leaching efficiency of metals was not much different between 3M (98.04% for lithium and 99.02% for cobalt) and 4M (98.89% for lithium and 98.54% for cobalt). Hence, 3 mol/L of sulphuric acid concentration was chosen to minimize risk of handling high concentrated acid, reduce cost as well as for environmental benefits. Refer to Table A.2 in Appendix A for detailed results.

4.3.2 Effect of reducing agent type and its concentration on metal leaching

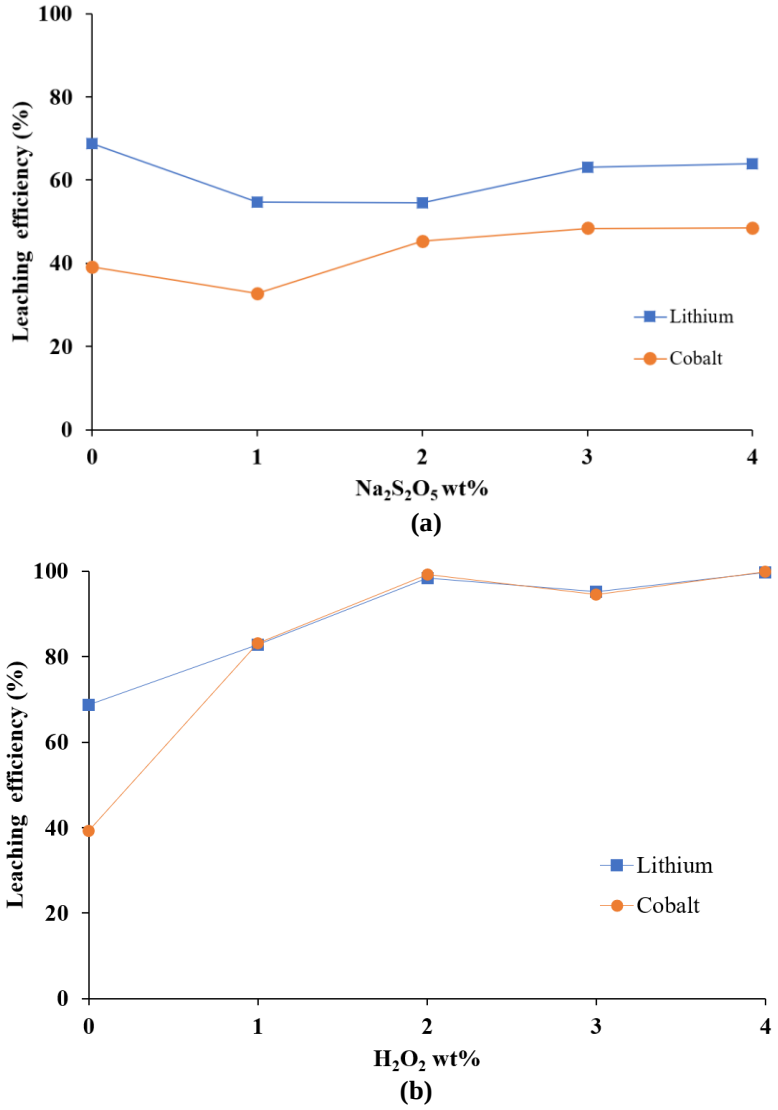

Figure 4.6 – Effect of reducing agent concentration
(a) $Na_2S_2O_5$ dosage; (b) H_2O_2 dosage
[2M H_2SO_4; Temperature: 40 ºC; Time: 2 hours; Pulp density: 20 g/L]

Presence of reducing agent in leaching mixture is for reducing Co^{3+} to Co^{2+}, which is leachable in sulphuric acid, hence, its presence could support efficiently for acid leaching process [74, 75]. $Na_2S_2O_5$ and H_2O_2 were studied at different concentration ranging from 0 % to 4 wt%.

Co and Li leaching efficiency vary significantly with different reducing agent types and concentrations. In absence of reducing agent, only 39.19% of Co and 68.74% of Li were leached from LCO powder. Addition of $Na_2S_2O_5$ up to 4 wt%. created no considerable leaching improvement when Co leaching efficiency reached 48.43 % and Li leaching efficiency even decreased to 63.11 % (Figure 4.6 - (a)). Whereas, addition of hydro peroxide

(from 0 to 4 wt%) increase leaching efficiency of Li and Co from 68.74 % and 39.19 % to 99.77% and 99.89%, respectively (Figure 4.6 - (b)).

H_2O_2 has a positive influence on metal recovery and is more appropriate for leaching step than $Na_2S_2O_5$ addition. In addition, 4 wt% H_2O_2 is optimal value of reducing agent concentration for better acid leaching of cathodic LCO powder. H_2O_2 was also chosen as reducing agent in other experiments for investigating the variation of other factors. Refer to Table A.3 in Appendix A for detailed results.

4.3.3 Effect of temperature on metal leaching

Metal leaching is considerably influenced by leaching temperature. Its effect on leaching efficiency was studied by changing leaching temperature. Figure 4.7 depicts that leaching efficiency of both lithium and cobalt increased with escalation of temperature. Increasing temperature results in providing energy for molecule movement and hence, there are more collision between LCO, sulphuric acid and hydro peroxide molecules [81]. Reaction, therefore, is facilitated due to more contact as well as collision of reactant molecules.

At room temperature (25 ^oC), only 79.65% of lithium and 76.31% of cobalt were leached while 99.26% lithium and 98.76% cobalt were recovered at 80 ^oC. Because no significant difference in metal leaching between 60 ^oC (99.11% Li and 99.69% Co) and 80 ^oC (99.26% Li and 98.76%), 60 ^oC is optimal value instead of 80 ^oC to minimize energy consumption of recycling process due to lower heating. Refer to Table A.4 in Appendix A for detailed results.

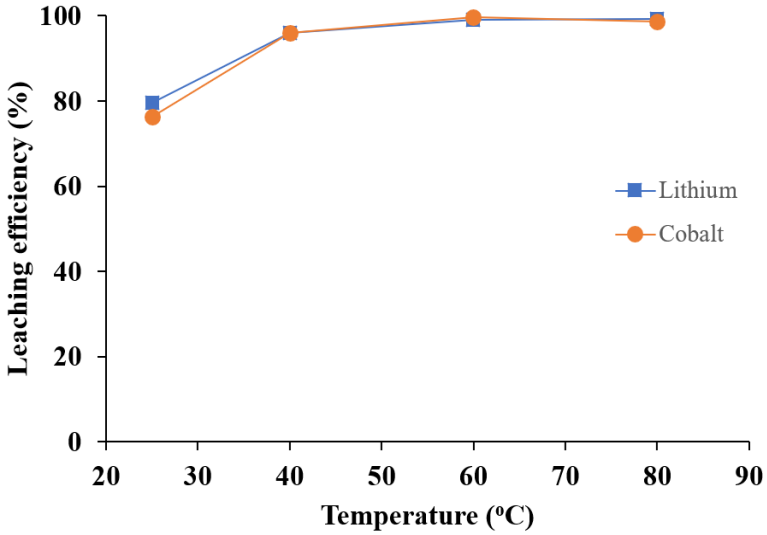

Figure 4.7 – Effect of temperature
[2 wt% H_2O_2; 2M H_2SO_4; Time: 2 hours; Pulp density: 20 g/L]

4.3.4 Effect of time on metal leaching

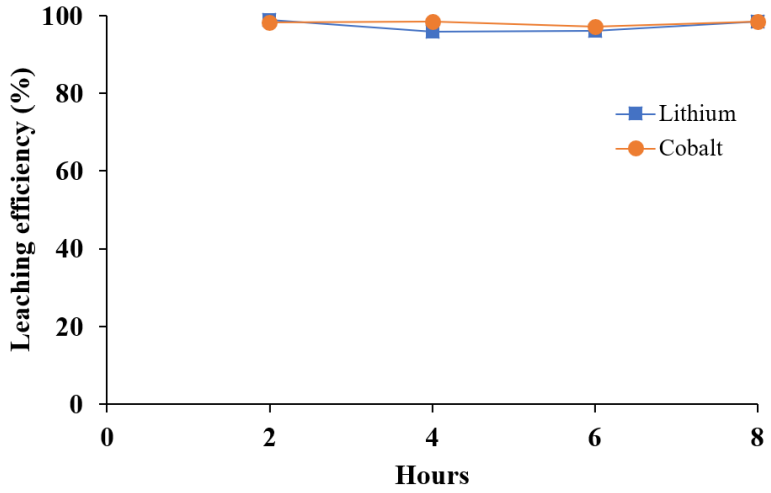

Figure 4.8 – Effect of time
[2 wt% H_2O_2; 2M H_2SO_4; Temperature: 40 ºC; Pulp density: 20 g/L]

Effect of leaching time on metal leaching was also researched by varying leaching time. Theoretically, leaching system requires sufficient time for reactant molecules having physical and chemical contact in order to achieve high leaching efficiency [81]. Results (Figure 4.8) show that rate of metal dissolution changed slightly as varying leaching time from 2 hours (98.84% Li and 98.19% Co) to 8 hours (98.49% Li and 98.51% Co). This means 2 hours is sufficient for metal leaching from LCO powder. Therefore, 2 hours is optimal value for leaching time parameter instead of leaching longer to reduce energy consumption and save time. Refer to Table A.5 in Appendix A for detailed results.

4.3.5 Effect of pulp density on metal leaching

Leaching efficiency of metals is dependent on pulp density since the dissolution of metals is also determined by the accessible surface area per unit volume of solution. Pulp density varies from 10 to 40 g/L. As shown in Figure 4.9, the leaching efficiency of lithium and cobalt change inversely to pulp density increase. At 10 g/L pulp density, 82.25% Li and 77.61% Co were leached, however, at 40 g/L pulp density, leaching efficiency of lithium and cobalt decrease to 82.05% and 79.25%, respectively. This phenomenon comes from the decrease of available surface area per unit volume in solution as pulp density increase [8]. Because of that, molecule contact reduces and mass transfer is limited, hence, chemical reaction is partially inhibited and leaching efficiency decreases [76]. The leaching efficiency reach peaks at 96.12% for Li and 97.53% for Co at 20 g/L pulp density before starting dropping at higher pulp density. In addition, low pulp density results in the increase of

leaching solution volume, which should be avoided in order to reduce waste quantity of recycling process [76]. Therefore, 20 g/L was considered appropriate for process optimization. Refer to Table A.6 in Appendix A for detailed results.

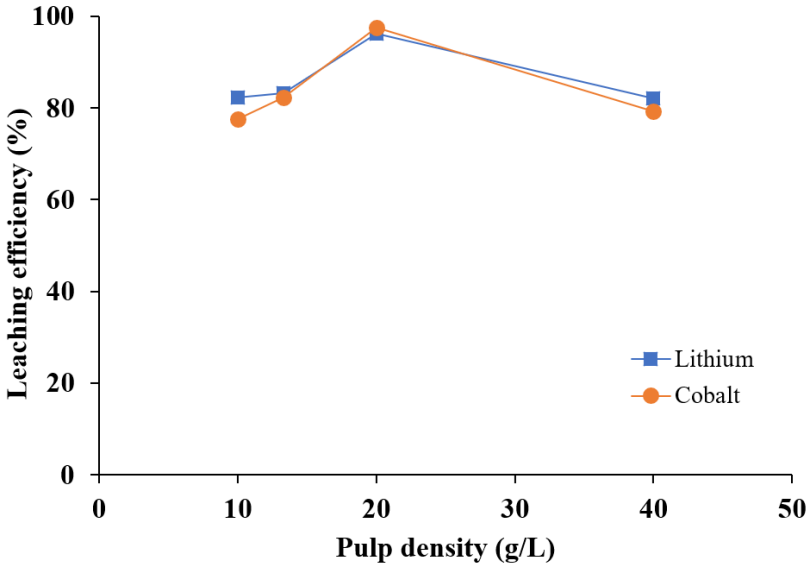

Figure 4.9 – Effect of pulp density
[2 wt% H_2O_2; 2M H_2SO_4; Temperature: 40 °C; Time: 2 hours]

Overall, through parameter investigations, leaching efficiency of Li and Co would reach optimization using 3 mol/L H_2SO_4 with presence of 4 wt% H_2O_2 at 20 g/L pulp density and 60 °C for 2 hours.

4.4 Selective precipitation to recover desired metals

The initial liquid for the selective precipitation is achieved as the leachate from optimal acid leaching of 1gram cathodic material. The achieved leachates are transparent and have pale red colour, which proves for the high presence of Co^{2+} [82]. Figure 4.10 shows experimental results of this stage.

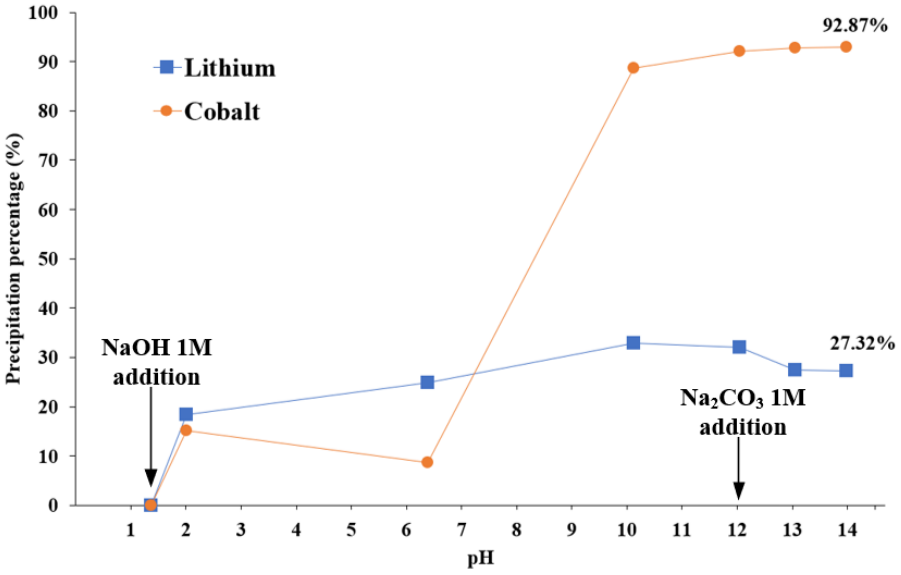

(a)

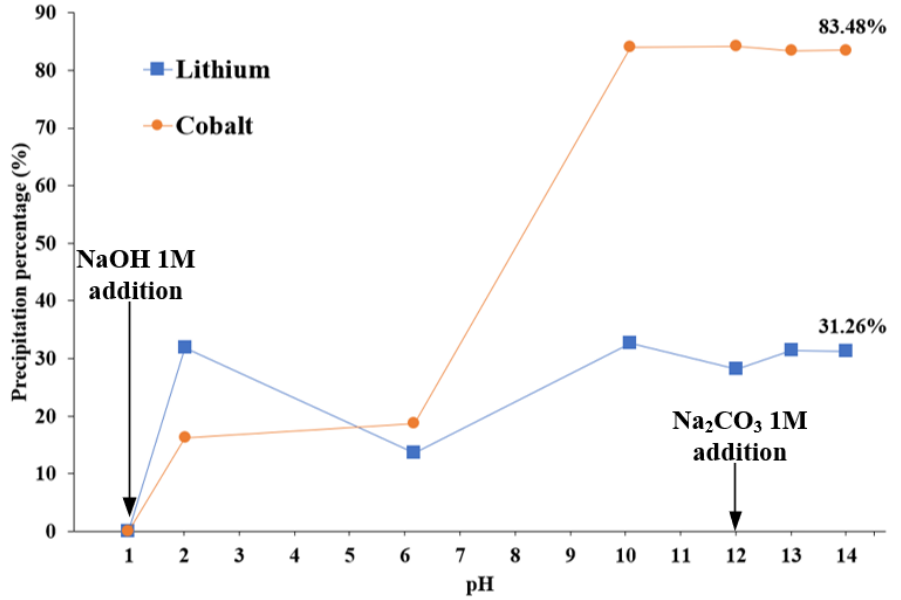

(b)

Figure 4.10 – Experimental results of Selective precipitation stage (a) first try. (b) second try.

Table 4.3 – Summary of recovery efficiency through two times try

Try	Metal	Leaching efficiency (%)	Precipitation efficiency (%)	Overall recovery efficiency (%)
1st	Lithium	99.11	27.32	27.08
	Cobalt	99.27	92.87	92.19
2nd	Lithium	99.36	31.26	31.06
	Cobalt	99.17	83.48	82.79

As shown in Figure 4.10 and Table 4.3, addition of NaOH 1M to increase pH to 12 separates over 80% of cobalt from achieved leachate (92.19% in first try and 82.79% in second try). However, the precipitation efficiency of lithium through two times is only 27.08% and

31.06%, respectively. Averaged overall recovery efficiency of lithium and cobalt are 29.07% and 87.49%, respectively (Calculated from Table 4.3). Refer to Appendix B for detailed result.

From Figure 4.10, it can be recognised that the precipitation of cobalt in achieved leachate starts at pH ≈ 2. This means Co^{3+} presents in achieved leachate because Figure 3.2 shows that only Co^{3+} precipitates once pH of solution exceeds 2. The formation of Co^{3+} in leachate could result from re-oxidation of Co^{2+} to Co^{3+} due to interaction with sulfur of sulphuric acid in alkaline environment (addition of NaOH 1M) [83]. This phenomenon only occurs at pH of 9-11 [83]. However, before NaOH is mixed and distributed well in solution, the addition of NaOH could cause local rapid increase of pH at some positions in solution. These positions are where re-oxidation phenomenon can quickly happen though overall pH of solution is still remaining low.

Overall, the precipitation of cobalt in pH = 2 to 6 did not exceed 20% and only increases significantly to above 80% as pH exceeds 9 before reaching precipitation peak at pH ≈ 12. This means amount of Co^{3+} is minor and Co^{2+} is still primary state of this metal in achieved leachate. As pH is above 12, cobalt precipitation stops growing and be stable. It can be explained as Co^{2+} stops precipitating and forms complex compounds in high pH environment as shown in Figure 3.2 – (a).

In terms of lithium, contrasting with theoretical Figure 3.2 – (b), experiment results show that lithium precipitation occurs from pH = 2 to 12 without addition of Na_2CO_3 (Figure 4.10). This phenomenon could result from the precipitation of cobalt from solution. Since cobalt precipitates and was separated from solution, lithium hydroxide molecules were stuck in cobalt precipitates and involved in filtrated precipitates. It results in decrease of lithium concentration in solution (27.32% in first try and 31.26% in second try) instead of actual chemical precipitation of lithium. This explanation becomes more evident as above pH = 12, with addition of Na_2CO_3 1M. At this point, lithium concentration is stable (precipitation efficiency does not increase) as cobalt stops precipitating from solution.

From pH = 12 to 14, lithium ions remaining in solution, in fact, were not precipitated by adding Na_2CO_3 1M. It can due to low temperature of precipitation stage (i.e. carried out at room temperature). Li_2CO_3 precipitate has solubility inversely proportional to temperature

[84]. Li_2CO_3 become less soluble at high temperature. Therefore, lithium precipitation as carbonates should be conducted at high temperature (i.e. above 90 ^oC [84]) for high precipitation efficiency.

Through experimental results, selective precipitation is not sufficient for separating and recovering lithium and cobalt from achieved leachate. Despite the significant difference of precipitation efficiency between lithium and cobalt (Table 4.3), the initial target at selective separating these metals from each other and from leachate is not achieved. In this stage, the addition of Na_2CO_3 to precipitate lithium ion does not work as theoretical hypothesis. Therefore, the precipitation efficiency of lithium (Figure 4.10 and Table 4.3) primarily results from lithium ions, which is stuck and mixed in cobalt precipitates achieved from leachate. It means the achieved precipitates from this stage are mixture of lithium and cobalt hydroxides rather than separated precipitates as expected.

From these experimental results, solvent extraction should be used to selectively extract and separate lithium or cobalt from leachate (i.e. commonly extract cobalt by P507, Cyanex 272 or PC-88A [84]. Refer to Table 2.5 for more details of these organic chemical systems). However, because solvent extraction can only selectively extract metal ions in organic liquid state, selective precipitation is required to recover both of them as solid products. Therefore, for optimal separation of these metals from leachate and from each other, a metal recovery stage, including a combination of solvent extraction and selective precipitation, is necessary. This means, for an optimal metal recovery stage, solvent extraction and selective precipitation should be combined. The former is to extract exclusively each metal from leachate while the latter is used to form recover products in solid state.

4.5 Cathodic material resynthesis

The precipitated mixture of hydroxides was calcined in laboratory calcination furnace at approximately 600-700 ^oC in 24h. The resulting solid sample was analysed by SEM-EDS and XRD to study its characterization. The SEM images (Figure 4.11 – (a) and (b)) show presence of large-sized particles in the recycled solid, in contrast to the particles of spent LCO powder extracted from spent battery cathode, in which smaller sizes and rounded shapes were observed (Figure 4.4). In addition, the EDS analysis (Figure 4.11 – (c)) provides high presence of Co and Oxygen as well. However, the high formation of large particles as well as high presence of cobalt and oxygen in recycled sample are not sufficient for

conclusion of LCO formation. A mixture of lithium and cobalt hydroxides can also provide similar EDS analysis result. Therefore, to guarantee the formation of LCO in recycled powder, XRD analysis is necessary to determine the presence of LCO through an instinctive characteristic of substance – its crystal structure.

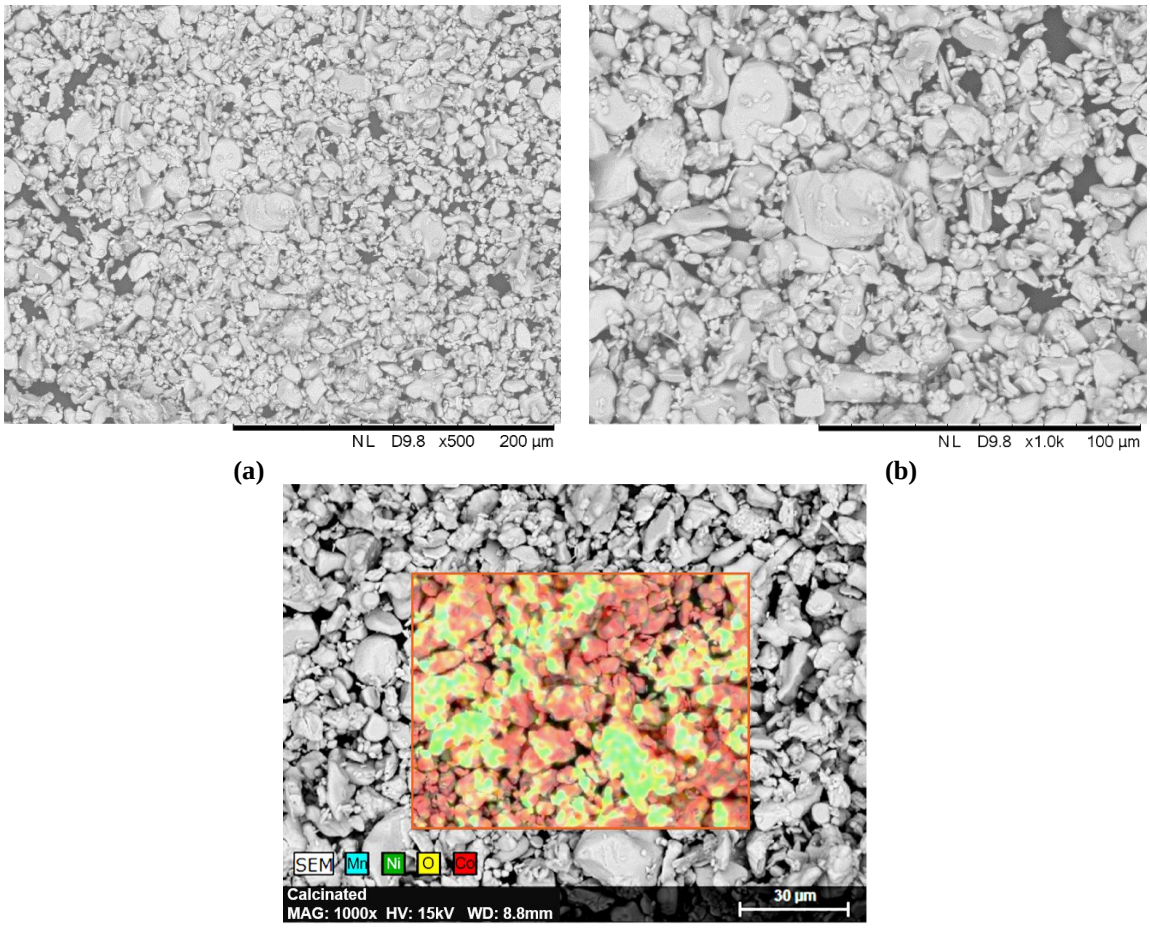

(a) **(b)** **(c)**

Figure 4.11 – SEM images of recycled precipitates
(a) At 500x magnification. (b) At 1000x magnification. (c) EDS analysis

The XRD result (Figure 4.12) depicts the XRD pattern of recycled LCO and commercial LCO powder. From XRD result, it can be seen that the recycled sample have peaks that fit with major peaks of standard LCO (at 2θ = 18.931°, 37.328°, 39.103°, 45.354°, 49.408°, 59.604°, 65.378°, 66.176°, 69.739°). The other noise peaks could be due to the presence of remaining cobalt hydroxide or cobalt oxide (Co_3O_4 – major calcined product of cobalt hydroxide [79]) or lithium hydroxide in the recycled powder. Comparing to commercial LCO powder, the recycled sample has similar characteristic peaks for the presence of LCO. The peak intensity difference of them could come from the purity as well as the extent of LCO formation reaction in the recycled sample.

In terms of LCO formation in the recycled sample, the achieved precipitate is primarily a mixture of lithium and cobalt hydroxides not separated precipitates of Li_2CO_3 and $Co(OH)_2$ as expected. However, the LCO was still achieved after the calcination of the precipitate. The mechanism of LCO formation in this case could come from the solid-state reaction between LiOH and $Co(OH)_2$ as following chemical reaction [85].

$$LiOH(s) + Co(OH)_2(s) + 0.5O_2(g) \rightarrow LiCoO_2(s) + 1.5H_2O(g)$$

Because the amount of cobalt and lithium in the achieved precipitate is significantly different (> 80% cobalt precipitated while only approximately 30% lithium precipitated), the solid-state reaction for LCO formation becomes dependent on the minor reactant – lithium hydroxides. Therefore, the formation of LCO in recycled sample occurred as below reaction but at very low conversion as reaction yield. The low conversion and reaction yield mean low amount of LCO formed after calcination. The low LCO yield and impurities are possibly attributed to the low intensity of peaks in recycled sample comparing to those in commercial LCO.

Overall, the XRD peaks of recycled LCO has high similarity to XRD pattern of standard LCO. Because each X-ray diffraction pattern is unique and only characteristic for a specific substance, this is the qualitative evidence for the formation and presence of LCO in the recycled sample. Therefore, it was then used as cathodic material to fabricate a new LIB.

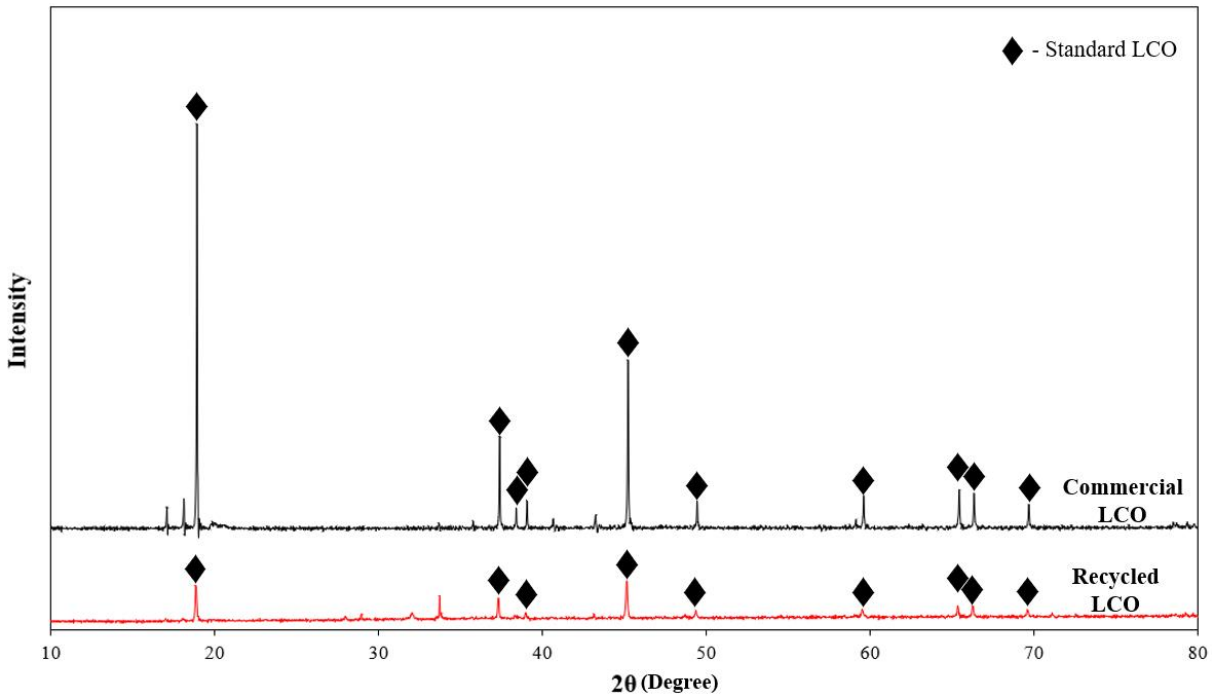

Figure 4.12 – XRD result of recycled LCO and commercial LCO

4.6 Fabrication of new lithium-ion battery from recovered product

Two different LIB coin cells were made – one with the recycled LCO material and the other with the commercial LCO powder. Electrochemical performance tests were conducted on both LIBs. As the anode and electrolyte are identical for the two batteries, the difference in their cycling performance is primarily due to the different cathodic materials – recycled LCO and commercial LCO.

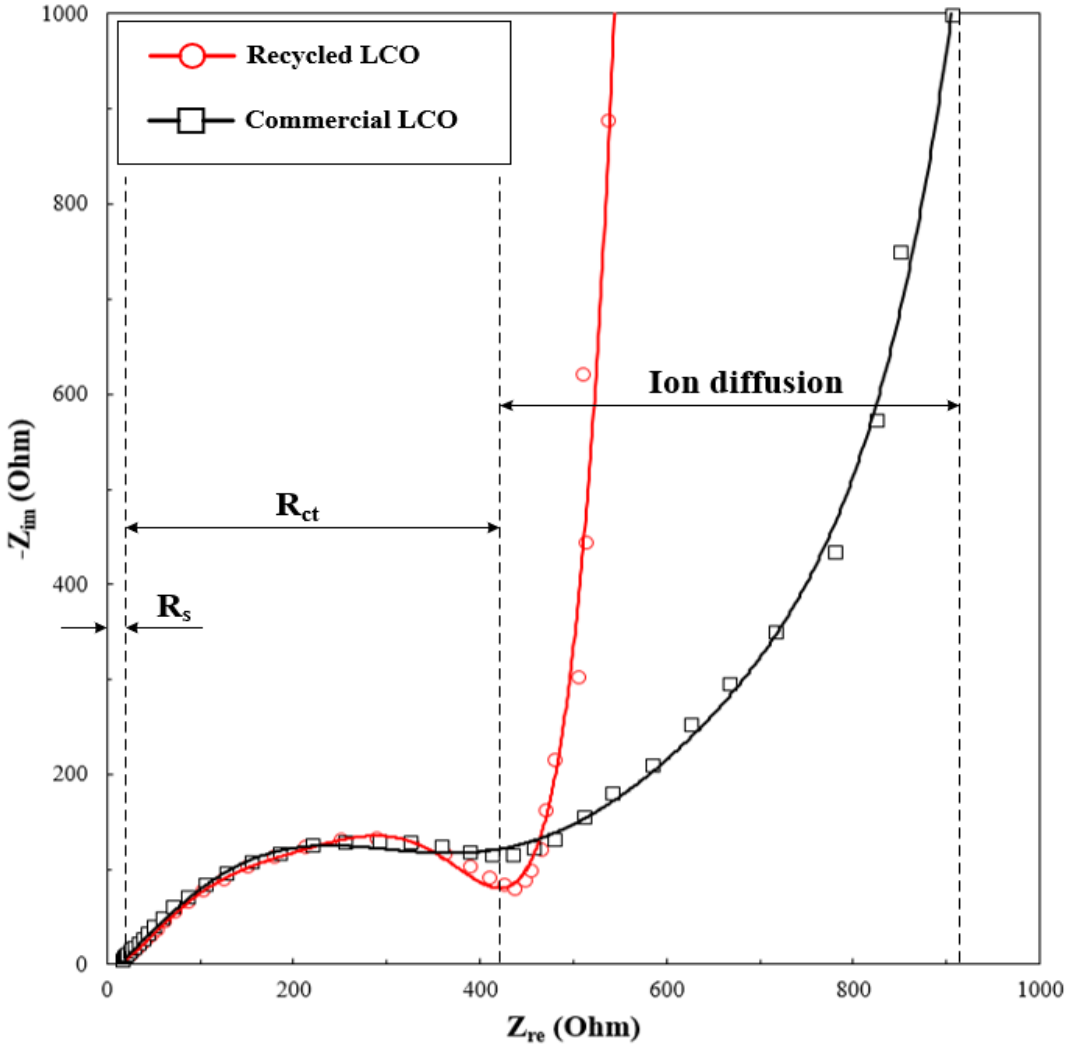

Figure 4.13 – Electrochemical impedance spectra (EIS) of fabricated batteries

Figure 4.13 presents the EIS of the two assembled batteries. The EIS test is used to study the response of an electrochemical cell to an applied AC potential. The result can be used to understand the different mechanisms (capability of impeding electron movement) in an electrochemical system. In this case, because the anode, electrolyte as well as current collectors of two batteries are identical, any changes in the EIS, primarily provides

information about the different kinetics between the cathodic materials – recycled LCO and commercial LCO.

From Figure 4.13, both impedance curves of two batteries include a semicircle and a line. The start of the semicircle intersects with x-axis, which represents for electrolyte resistance (R_s) [86]. The R_s is similar for the two batteries (21.3 Ω for recycled LCO, 20.6 Ω for commercial LCO). The semicircle component is ascribed to the charge transfer kinetics (R_{ct}) [86]. There is no discernible difference in the shape of the semicircle for the two batteries. As such, it is concluded that the charge transfer resistance of two batteries is similar.

The lines following the semicircles are where the major differences are observed. This line in the low frequency region is attributed to the ion diffusion kinetics in the batteries [86, 87]. The recycled LCO sample has a steeper line than the commercial LCO. Although a steep line is often considerable an indication of a low diffusion resistance, in this case the low frequency component of the recycled LCO is almost straight. This suggests that there may be a pure capacitive response at these low frequencies for the recycled LCO. The response from the commercial LCO is characteristic of typical diffusion response. In conclusion, the battery electrolyte resistance and charge transfer kinetics look similar, but the diffusion response is very different.

Figure 4.14 shows the cycling performance of two batteries when discharging at 0.5C (80 $mA.g^{-1}$ current density) at room temperature. The commercial LCO battery exhibits a better performance than the recycled LCO battery. The initial capacity of the commercial LCO battery is approximately 120 $mAh.g^{-1}$. The capacity decays to approximately 85 $mAh.g^{-1}$ after 40 cycles.

The recycled LCO battery shows a very low irreversible specific capacity of 6.7 $mAh.g^{-1}$, which rapidly drops to 0.4 $mAh.g^{-1}$ after 3 cycles. The poor cycling performance of the recycled LCO battery is attributed to the poor intercalation and de-intercalation of lithium ions into the layered LCO structure. Although the XRD from for the recycled LCO looks good, it may be impurities from the recycling process that are inhibiting the Li ion intercalation and leads to poor cycling performance.

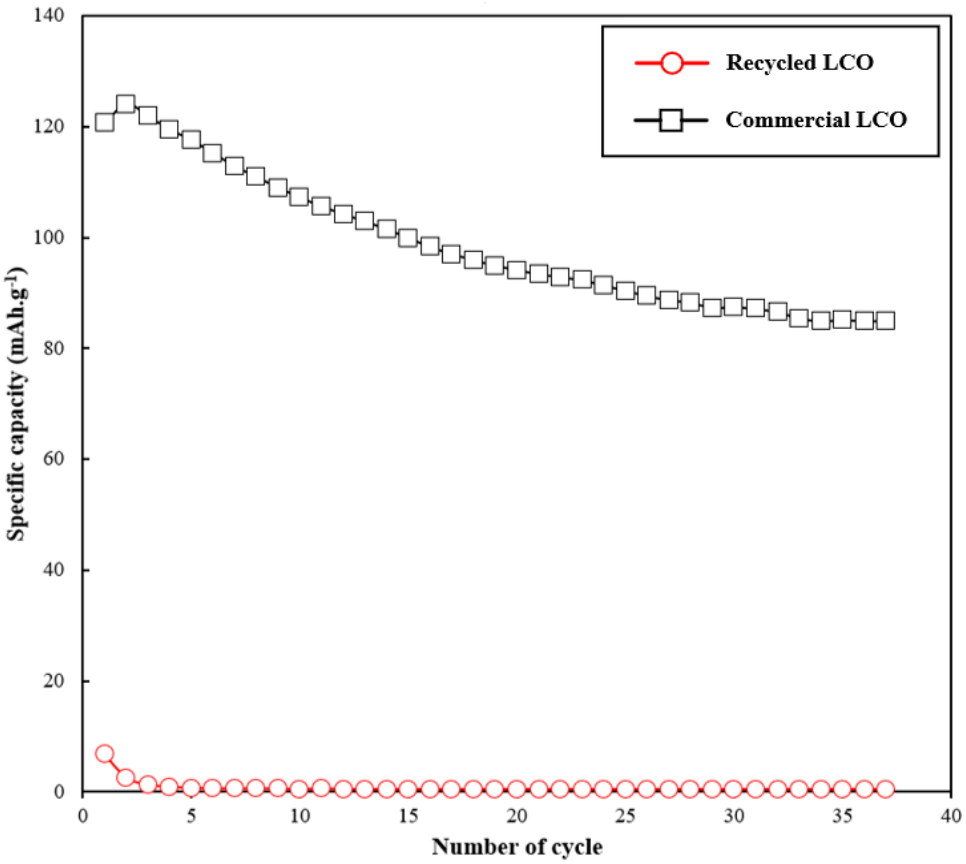

Figure 4.14 – Cycling performance of fabricated batteries

Overall, the recycled LCO show poor electrochemical performance comparing to commercial LCO. It has similar electrolyte resistance and charge transfer kinetics to the commercial LCO. However, the recycled LCO shows a higher capacitance behaviour than the commercial LCO. In terms of cycling performance, while commercial LCO has high specific capacity (120 $mAh.g^{-1}$) and a good cycling stability, the recycled LCO provided a very low irreversible specific capacity of 6.7 $mAh.g^{-1}$. Its capacity was also rapidly faded to approximately 0.4 $mAh.g^{-1}$ after 3 cycles. The impurities (e.g. lithium and cobalt oxides, hydroxides and other metals) as well as low yield of LCO formation in recycled LCO could be reasons to inhibit the intercalation of lithium ions. Hence, they lead to the poor electrochemical performance of recycled LCO.

5 CONCLUSION

5.1 Achievements

The key players in the LIB recycling market have been highlighted as Umicore, Toxco and INMETCO. However, there is still a gap in these recycling process with some processing being expensive or not recovering key materials such as Li. Most of these processes waste highly valuable components and only recovers the spent LIBs as cheap products. Therefore, enhancing quality of recycled products (i.e. recovering valuable components) can increase profit and attract more investment for the spent LIBs recycling.

The methods for leaching the key metals from the spent batteries have been critically analysed and the process has been optimised in the current study. The optimization was conducted by varying the leaching conditions to study each condition effect on the acid leaching stage. From that, the optimal conditions were identified for optimal leaching efficiency of lithium and cobalt with lowest energy and time consumption. The optimal leaching efficiency of lithium and cobalt can be achieved through the acid leaching conducted in 3M H_2SO_4, 4 wt% H_2O_2, in 2 hours at 60 ^oC and 20 g/L pulp density. These leaching factors guarantee over 99% of lithium and cobalt leached from the LCO powder. This is amongst the high leaching efficiencies reported in Literature Review. In addition, this is also the leaching scheme with the highest efficiency at the lowest temperature. Most of leaching schemes reported in section 2.2.2 requires at least 80 ^oC for high leaching efficiency, whilst the leaching scheme in this study is only at 60 ^oC for over 99% of lithium and cobalt leaching efficiency.

The selective precipitation by using NaOH and Na_2CO_3 was executed to selectively separate Co and Li ions from the leachate of optimal acid leaching. The overall precipitation efficiency of cobalt is over 80%. The lithium precipitation efficiency from the leaching solution is over 27% but primarily came from the co-precipitation with cobalt. The lithium precipitation did not happen due to the addition of Na_2CO_3 as expected. Hence, the achieved precipitate is a mixture of lithium and cobalt hydroxides rather than separated precipitate of each metals. This result show average level of metal recovery efficiency from leaching solutions comparing to studies summarised in the Literature Review. Therefore, further studies and improvements are required to enhance the recovery efficiency of key metals are necessary.

The precipitated product was calcined to form LCO through solid-state reaction. The XRD result show presence of LCO in the recycled sample due to its XRD peak similarity to XRD pattern of standard LCO. Therefore, the recycled LCO was used as cathodic material for fabricating LIB coin cell. In comparison with the assembled commercial LCO battery, the fabricated recycled LCO battery shows a similar electrolyte resistance and charge transfer characteristic but unfortunately a poor battery performance. The initial capacity of the commercial LCO battery is approximately 120 $mAh.g^{-1}$. Its capacity decays to approximately 85 $mAh.g^{-1}$ after 40 cycles. The recycled LCO battery has a low irreversible specific capacity (6.7 $mAh.g^{-1}$) and rapidly faded to 0.4 $mAh.g^{-1}$ after only 3 cycles. This is attributed to the impurities as well as low yield of LCO formation in recycled LCO. They significantly impact on the intercalation/de-intercalation of lithium ions, which is required for LIB operation.

5.2 Remaining issues and recommendations for future works

The project still has issues and therefore, requires further works to solve and improve. These followings are remaining issues and the corresponding recommendations for solving these issues.

- **Issue 1:** Limitation of feedstock source;
- **Recommendations**: The spent LIBs studied in this thesis only come from iPhone. Therefore, to guarantee the flexibility of the recycling scheme, the source of spent LIBs for recycling scheme should be diversified. Spent LIBs from laptop, digital cameras or other smartphone brands (e.g. Samsung, Oppo or Nokia) should be collected for recycling.

- **Issue 2:** Corrosive and dangerous leaching solution of acid leaching stage;
- **Recommendations**: Although the acid leaching stage was optimised for maximal leaching efficiency of lithium and cobalt, the leaching system of it still propose some dangers and aggressive environment, which can increase the intensity of post-treatment. The H_2SO_4-H_2O_2 system is commonly called 'Piranha solution', which is extremely corrosive and powerfully oxidising. However, the recycling scheme for spent LIB aims at mild and eco-friendly conditions, which can reduce the post-treatment intensity for acid leaching as well as the risks of handling with high-concentrated chemicals. Therefore, research for less concentrated acid medium with

similar leaching efficiency should be conducted for optimising the eco-friendliness of the recycling scheme.

- **Issue 3:** Selective precipitation is not sufficient to separate lithium and cobalt from the leaching solution and from each other;
- **Recommendations:** The experiment results showed that the achieved precipitate is a mixture of lithium and cobalt hydroxides rather than separated precipitates (Li_2CO_3 and Co_3O_4) as planned. Therefore, a combination of solvent extraction and selective precipitation should be studied to enhance the separation efficiency. The former is to extract exclusively each metal from leachate while the latter is used to form recover products in solid state. The enhanced separation efficiency can subsequently result in higher quality of synthesized LCO and therefore, LIBs fabricated from recycled LCO can produce higher electrochemical performance, especially its specific capacity. This, as a result, provides better practical feasibility for the recycling scheme.

- **Issue 4:** Low number of cycles at only one discharge rate in the cycling performance test;
- **Recommendations:** Due to time limitation for the thesis as well as long duration required for a comprehensive cycling performance test, the cycling performance test in this thesis only conducted 37 charge-discharge cycles at only 0.5C in room condition. For cycling performance tests in the future, it should be conducted at higher number of cycles at different charge/discharge rate. This is to study comprehensively the electrochemical performance of a LIB fabricated from recycled products. Therefore, in-depth evaluations in terms of overall efficiency of recycling scheme could be achieved.

6 REFERENCES

[1] Zubi, G., Dufo-López, R., Carvalho, M., and Pasaoglu, G. (2018). The lithium-ion battery: State of the art and future perspectives, *Renewable and Sustainable Energy Reviews 89*, 292-308.

[2] Liu, C., Neale, Z. G., and Cao, G. (2016). Understanding electrochemical potentials of cathode materials in rechargeable batteries, *Materials Today 19*, 109-123.

[3] Pillot, C. (2017). The rechargeable battery market and main trend 2016-2025, Avicenne Energy.

[4] Desjardins, J. (2016). Explaining the Surging Demand for Lithium-Ion Batteries <https://www.visualcapitalist.com/explaining-surging-demand-lithium-ion-batteries/>, Visual Capitalist.

[5] Zeng, X., Li, J., and Singh, N. (2014). Recycling of Spent Lithium-Ion Battery: A Critical Review, *Critical Reviews in Environmental Science and Technology 44*, 1129-1165.

[6] Zheng, X., Zhu, Z., Lin, X., Zhang, Y., He, Y., Cao, H., and Sun, Z. (2018). A Mini-Review on Metal Recycling from Spent Lithium Ion Batteries, *Engineering 4*, 361-370.

[7] Natarajan, S., and Aravindan, V. (2018). Recycling Strategies for Spent Li-Ion Battery Mixed Cathodes, *ACS Energy Letters 3*, 2101-2103.

[8] Dutta, D., Kumari, A., Panda, R., Jha, S., Gupta, D., Goel, S., and Jha, M. K. (2018). Close loop separation process for the recovery of Co, Cu, Mn, Fe and Li from spent lithium-ion batteries, *Separation and Purification Technology 200*, 327-334.

[9] InfoMine. (2019). 1 Year Cobalt Prices and Price Charts, InfoMine.

[10] Elwert, T., Goldmann, D., Römer, F., Buchert, M., Merz, C., Schueler, D., and Sutter, J. (2015). Current Developments and Challenges in the Recycling of Key Components of (Hybrid) Electric Vehicles, *Recycling 1*, 25.

[11] Li, L., Zhang, X., Li, M., Chen, R., Wu, F., Amine, K., and Lu, J. (2018). *The Recycling of Spent Lithium-Ion Batteries: a Review of Current Processes and Technologies*.

[12] Whittingham, M. S. (1976). Electrical energy storage and intercalation chemistry, *Science 192*, 1126-1127.

[13] Besenhard, J. O., and Schöllhorn, R. (1976). The discharge reaction mechanism of the MoO3 electrode in organic electrolytes, *Journal of Power Sources 1*, 267-276.

[14] Besenhard, J. O. (1976). The electrochemical preparation and properties of ionic alkali metal- and NR4-graphite intercalation compounds in organic electrolytes, *Carbon 14*, 111-115.

[15] Basu, S., Zeller, C., Flanders, P. J., Fuerst, C. D., Johnson, W. D., and Fischer, J. E. (1979). Synthesis and properties of lithium-graphite intercalation compounds, *Materials Science and Engineering 38*, 275-283.

[16] Yazami, R., and Touzain, P. (1983). A reversible graphite-lithium negative electrode for electrochemical generators, *Journal of Power Sources 9*, 365-371.

[17] Mahmood, N., and Hou, Y. (2014). Electrode Nanostructures in Lithium-Based Batteries, *Advanced science (Weinheim, Baden-Wurttemberg, Germany) 1*, 1400012.

[18] Heelan, J., Gratz, E., Zheng, Z., Wang, Q., Chen, M., Apelian, D., and Wang, Y. (2016). Current and Prospective Li-Ion Battery Recycling and Recovery Processes, *JOM 68*, 2632-2638.

[19] Desjardins, J. (2017). The Cathode is the Key to Advancing Lithium-Ion Technology <https://www.visualcapitalist.com/cathode-advancing-lithium-ion/>, Visual Capitalist.

[20] Blomgren, G. E. (2017). The Development and Future of Lithium Ion Batteries, *Journal of The Electrochemical Society 164*, A5019-A5025.

[21] Yoshino, A. (2014). 1 - Development of the Lithium-Ion Battery and Recent Technological Trends, In *Lithium-Ion Batteries* (Pistoia, G., Ed.), pp 1-20, Elsevier, Amsterdam.

[22] Shen, X., Tian, Z., Fan, R., Shao, L., Zhang, D., Cao, G., Kou, L., and Bai, Y. (2018). Research progress on silicon/carbon composite anode materials for lithium-ion battery, *Journal of Energy Chemistry 27*, 1067-1090.

[23] Lim, J.-E., Kim, J., Kim, Y., and Kim, J.-K. (2018). Binder-free hybrid Li4Ti5O12 anode for high performance lithium-ion batteries, *Electrochimica Acta 282*, 270-275.

[24] Ren, Y. H., Wu, B. R., Yang, C. W., Wu, F., and Chen, F. B. (2011). Review of new lithium slats of electrolyte for Li-ion batteries, *Chin J Power Sources 35*, 1171-1174.

[25] Domi, Y., Doi, T., Ochida, M., Yamanaka, T., Abe, T., and Ogumi, Z. (2016). Intercalation/De-Intercalation Reactions of Lithium Ion at Graphite in Electrolyte Solutions Containing 3D-Transition-Metal Ions and Cyclic Ethers, *Journal of The Electrochemical Society 163*, A2849-A2853.

[26] Winslow, K. M., Laux, S. J., and Townsend, T. G. (2018). A review on the growing concern and potential management strategies of waste lithium-ion batteries, *Resources, Conservation and Recycling 129*, 263-277.

[27] Taniguchi, I. (2015). Olivine-Type Cathode Materials for Lithium-Ion Batteries <https://www.sigmaaldrich.com/technical-documents/articles/materials-science/olivine-type-cathode-materials.html>, Sigma-Aldrich.

[28] Bernardes, A. M., Espinosa, D. C. R., and Tenório, J. A. S. (2004). Recycling of batteries: a review of current processes and technologies, *Journal of Power Sources 130*, 291-298.

[29] Zhuang, W.-Q., Fitts, J. P., Ajo-Franklin, C. M., Maes, S., Alvarez-Cohen, L., and Hennebel, T. (2015). Recovery of critical metals using biometallurgy, *Current Opinion in Biotechnology 33*, 327-335.

[30] Georgi-Maschler, T., Friedrich, B., Weyhe, R., Heegn, H., and Rutz, M. (2012). Development of a recycling process for Li-ion batteries, *Journal of Power Sources 207*, 173-182.

[31] Gaines, L. (2018). Lithium-ion battery recycling processes: Research towards a sustainable course, *Sustainable Materials and Technologies 17*, e00068.

[32] M., P. (2018). Solvent Extraction: Definition & Process (https://study.com/academy/lesson/solvent-extraction-definition-process.html), study.com.

[33] Wang, R.-C., Lin, Y.-C., and Wu, S.-H. (2009). A novel recovery process of metal values from the cathode active materials of the lithium-ion secondary batteries, *Hydrometallurgy 99*, 194-201.

[34] Zhang, P., Yokoyama, T., Itabashi, O., Suzuki, T. M., and Inoue, K. (1998). Hydrometallurgical process for recovery of metal values from spent lithium-ion secondary batteries, *Hydrometallurgy 47*, 259-271.

[35] Castillo, S., Ansart, F., Laberty-Robert, C., and Portal, J. (2002). Advances in the recovering of spent lithium battery compounds, *Journal of Power Sources 112*, 247-254.

[36] Lee, C. K., and Rhee, K.-I. (2003). Reductive leaching of cathodic active materials from lithium ion battery wastes, *Hydrometallurgy 68*, 5-10.

[37] Lee, C., and Rhee, K.-I. (2002). *Preparation of LiCoO 2 from spent lithium-ion batteries*, Vol. 109.

[38] Li, L., Chen, R., Sun, F., Wu, F., and Liu, J. (2011). Preparation of LiCoO2 films from spent lithium-ion batteries by a combined recycling process, *Hydrometallurgy 108*, 220-225.

[39] Sun, L., and Qiu, K. (2011). Vacuum pyrolysis and hydrometallurgical process for the recovery of valuable metals from spent lithium-ion batteries, *Journal of Hazardous Materials 194*, 378-384.

[40] Tanong, K., Coudert, L., Chartier, M., Mercier, G., and Blais, J.-F. (2017). Study of the factors influencing the metals solubilisation from a mixture of waste batteries by response surface methodology, *Environmental Technology 38*, 3167-3179.

[41] Wang, J., Chen, M., Chen, H., Luo, T., and Xu, Z. (2012). Leaching Study of Spent Li-ion Batteries, *Procedia Environmental Sciences 16*, 443-450.

[42] Zhu, S.-g., He, W.-z., Li, G.-m., Zhou, X., Zhang, X.-j., and Huang, J.-w. (2012). Recovery of Co and Li from spent lithium-ion batteries by combination method of acid leaching and chemical precipitation, *Transactions of Nonferrous Metals Society of China 22*, 2274-2281.

[43] Granata, G., Moscardini, E., Pagnanelli, F., Trabucco, F., and Toro, L. (2012). Product recovery from Li-ion battery wastes coming from an industrial pre-treatment plant: Lab scale tests and process simulations, *Journal of Power Sources 206*, 393-401.

[44] Kang, J., Senanayake, G., Sohn, J., and Shin, S. M. (2010). Recovery of cobalt sulfate from spent lithium ion batteries by reductive leaching and solvent extraction with Cyanex 272, *Hydrometallurgy 100*, 168-171.

[45] Li, L., Lu, J., Ren, Y., Zhang, X. X., Chen, R. J., Wu, F., and Amine, K. (2012). Ascorbic-acid-assisted recovery of cobalt and lithium from spent Li-ion batteries, *Journal of Power Sources 218*, 21-27.

[46] Li, L., Bian, Y., Zhang, X., Guan, Y., Fan, E., Wu, F., and Chen, R. (2018). Process for recycling mixed-cathode materials from spent lithium-ion batteries and kinetics of leaching, *Waste Management 71*, 362-371.

[47] Sun, L., and Qiu, K. (2012). Organic oxalate as leachant and precipitant for the recovery of valuable metals from spent lithium-ion batteries, *Waste Management 32*, 1575-1582.

[48] He, L.-P., Sun, S.-Y., Mu, Y.-Y., Song, X.-F., and Yu, J.-G. (2017). Recovery of Lithium, Nickel, Cobalt, and Manganese from Spent Lithium-Ion Batteries Using l-Tartaric Acid as a Leachant, *ACS Sustainable Chemistry & Engineering 5*, 714-721.

[49] Nayaka, G. P., Pai, K. V., Santhosh, G., and Manjanna, J. (2016). Dissolution of cathode active material of spent Li-ion batteries using tartaric acid and ascorbic acid mixture to recover Co, *Hydrometallurgy 161*, 54-57.

[50] Nayaka, G. P., Pai, K. V., Santhosh, G., and Manjanna, J. (2016). Recovery of cobalt as cobalt oxalate from spent lithium ion batteries by using glycine as leaching agent, *Journal of Environmental Chemical Engineering 4*, 2378-2383.

[51] Nan, J., Han, D., Yang, M., Cui, M., and Hou, X. (2006). Recovery of metal values from a mixture of spent lithium-ion batteries and nickel-metal hydride batteries, *Hydrometallurgy 84*, 75-80.

[52] Swain, B., Jeong, J., Lee, J.-c., Lee, G.-H., and Sohn, J.-S. (2007). Hydrometallurgical process for recovery of cobalt from waste cathodic active material generated during manufacturing of lithium ion batteries, *Journal of Power Sources 167*, 536-544.

[53] Pranolo, Y., Zhang, W., and Cheng, C. Y. (2010). Recovery of metals from spent lithium-ion battery leach solutions with a mixed solvent extractant system, *Hydrometallurgy 102*, 37-42.

[54] Suzuki, T., Nakamura, T., Inoue, Y., Niinae, M., and Shibata, J. (2012). A hydrometallurgical process for the separation of aluminum, cobalt, copper and lithium in acidic sulfate media, *Separation and Purification Technology 98*, 396-401.

[55] Gao, J.-m., Zhang, M., Cheng, F., and Guo, M. (2017). Process development for selective precipitation of valuable metals and simultaneous synthesis of single-phase spinel ferrites from saprolite-limonite laterite leach liquors, *Hydrometallurgy 173*, 98-105.

[56] Provazi, K., Campos, B. A., Espinosa, D. C. R., and Tenório, J. A. S. (2011). Metal separation from mixed types of batteries using selective precipitation and liquid–liquid extraction techniques, *Waste Management 31*, 59-64.

[57] Contestabile, M., Panero, S., and Scrosati, B. (2001). A laboratory-scale lithium-ion battery recycling process, *Journal of Power Sources 92*, 65-69.

[58] Bertuol, D. A., Bernardes, A. M., and Tenório, J. A. S. (2009). Spent NiMH batteries—The role of selective precipitation in the recovery of valuable metals, *Journal of Power Sources 193*, 914-923.

[59] Li, J., Shi, P., Wang, Z., Chen, Y., and Chang, C.-C. (2009). A combined recovery process of metals in spent lithium-ion batteries, *Chemosphere 77*, 1132-1136.

[60] Dorella, G., and Mansur, M. B. (2007). A study of the separation of cobalt from spent Li-ion battery residues, *Journal of Power Sources 170*, 210-215.

[61] Nayl, A. A., Elkhashab, R. A., Badawy, S. M., and El-Khateeb, M. A. (2017). Acid leaching of mixed spent Li-ion batteries, *Arabian Journal of Chemistry 10*, S3632-S3639.

[62] Chen, X., Xu, B., Zhou, T., Liu, D., Hu, H., and Fan, S. (2015). Separation and recovery of metal values from leaching liquor of mixed-type of spent lithium-ion batteries, *Separation and Purification Technology 144*, 197-205.

[63] Knights, B. D. H., and Saloojee, F. (2015). Lithium battery recycling, In *Green Economy research reports*, South Africa.

[64] Yan, J., and A. Nomeli, M. (2015). *Handbook of Clean Energy Systems, 6 Volume Set*.

[65] Donald L. Stewart, J., James C. Daley, Robert L. Stephens (2000). *Fourth International Symposium on Recycling of Metals and Engineered Materials*, Wiley.

[66] Egerton, R. F. (2016). *Physical Principles of Electron Microscopy An Introduction to TEM, SEM, and AEM*, 2nd ed. 2016.. ed., Cham : Springer International Publishing : Imprint: Springer.

[67] Goldstein, J. I., Newbury, D. E., Michael, J. R., Ritchie, N. W. M., Scott, J. H. J., and Joy, D. C. (2018). *Scanning Electron Microscopy and X-Ray Microanalysis*, Springer New York: New York, NY.

[68] Goodge, J. (2017). Energy-Dispersive X-Ray Spectroscopy (EDS), https://serc.carleton.edu/research_education/geochemsheets/eds.html.

[69] Levenson, R. (2001). *More Modern Chemical Techniques*, Royal Society of Chemistry.

[70] InTech (2012). *Atomic Absorption Spectroscopy* InTechweb.org.

[71] Stephen R Byrn, G. Z., Xiaoming (Sean) Chen (2017). *Solid State Properties of Pharmaceutical Materials*, 1st ed., John Wiley and Sons Inc.

[72] Zolotoyabko, E. (2014). *Basic concepts of X-ray diffraction*, Weinheim : Wiley-VCH.

[73] Dykes, B. (2018). The Recycling of Lithium-ion Batteries In *School of Mechanical and Mining Engineering*, The University of Queensland, Australia.

[74] Miamari Aaltonen, C. P., Benjamin P. Wilson ID and Mari Lundström. (2017). Leaching of Metals from Spent Lithium-Ion Batteries, *Recyling 2*, 9.

[75] Li, L., Ge, J., Chen, R., Wu, F., Chen, S., and Zhang, X. (2010). Environmental friendly leaching reagent for cobalt and lithium recovery from spent lithium-ion batteries, *Waste Management 30*, 2615-2621.

[76] Meshram, P., Pandey, B. D., and Mankhand, T. R. (2015). Recovery of valuable metals from cathodic active material of spent lithium ion batteries: Leaching and kinetic aspects, *Waste Management 45*, 306-313.

[77] Choubey, P. K., Chung, K.-S., Kim, M.-s., Lee, J.-c., and Srivastava, R. R. (2017). Advance review on the exploitation of the prominent energy-storage element Lithium. Part II: From sea water and spent lithium ion batteries (LIBs), *Minerals Engineering 110*, 104-121.

[78] Garcia, E. M., Santos, J. S., Pereira, E. C., and Freitas, M. B. J. G. (2008). Electrodeposition of cobalt from spent Li-ion battery cathodes by the electrochemistry quartz crystal microbalance technique, *Journal of Power Sources 185*, 549-553.

[79] dos Santos, C. S., Alves, J. C., da Silva, S. P., Evangelista Sita, L., da Silva, P. R. C., de Almeida, L. C., and Scarminio, J. (2019). A closed-loop process to recover Li and Co compounds and to resynthesize LiCoO2 from spent mobile phone batteries, *Journal of Hazardous Materials 362*, 458-466.

[80] University, B. (2017). BU-303: Confusion with Voltages <https://batteryuniversity.com/index.php/learn/article/confusion_with_voltages>, batteryuniversity.com.

[81] Peters, B. (2017). *Reaction Rate Theory and Rare Events*, Netherlands: Elsevier.

[82] Zhao, H., Hao, J., Ban, Y., Sha, Y., Zhou, H., and Liu, Q. (2019). Novel and efficient cobalt catalysts synthesized by one-step solution phase reduction for the conversion of biomass derived ethyl levulinate, *Catalysis Today 319*, 145-154.

[83] Yuan, Y., Zhao, D., Li, J., Wu, F., Brigante, M., and Mailhot, G. (2018). Rapid oxidation of paracetamol by Cobalt(II) catalyzed sulfite at alkaline pH, *Catalysis Today 313*, 155-160.

[84] Kumar Choubey, P., Chung, K.-S., Kim, M.-s., Lee, J.-c., and Srivastava, R. R. (2017). *Advance review on the exploitation of the prominent energy-storage element Lithium. Part II: From sea water and spent lithium ion batteries (LIBs)*, Vol. 110.

[85] Sunandana, C. S. (2015). *Introduction to Solid State Ionics-Phenomenology and Applications,, ,2015*.

[86] Feng, M., Du, Q., Su, L., Zhang, G., Wang, G., Ma, Z., Gao, W., Qin, X., and Shao, G. (2017). Manganese oxide electrode with excellent electrochemical performance for sodium ion batteries by pre-intercalation of K and Na ions, *Scientific Reports 7*, 2219.

[87] Pham, T. N., Tanaji, S. T., Choi, J.-S., Lee, H. U., Kim, I. T., and Lee, Y.-C. (2019). Preparation of Sn-aminoclay (SnAC)-templated Fe3O4 nanoparticles as an anode material for lithium-ion batteries, *RSC Advances 9*, 10536-10545.

APPENDIX A – AAS ANALYSIS RESULTS OF ACID LEACHING

Table A.1 – AAS analysis of cathodic material components
[2 wt% H_2O_2; 3M H_2SO_4; Time: 4 hours; Temperature: 60 ºC; Pulp density: 20 g/L]

Sample ID	Cathodic material mass (gram)	[Li] (mg/L)	m_{Li} (gram)	[Co] (mg/L)	m_{Co} (gram)
Raw.LCO.1	0.499	1599	0.039975	12740	0.3185
Raw.LCO.2	0.501	1661	0.041525	13410	0.33525
Raw.LCO.3	0.5	1703	0.042575	13330	0.33325
Average	0.5		0.0414		0.329

Table A.2 – AAS results for acid concentration effect
[2 wt% H_2O_2; Time: 2 hours; Temperature: 40 ºC; Pulp density: 20 g/L]

Sample ID	LCO mass (gram)	Acid Concen. (mol/L)	[Li] (mg/L)	m_{Li} (gram)	% Li leached	[Co] (mg/L)	m_{Co} (gram)	% Co leached
AC1M	0.503	1	1243	0.031075	74.61	8953	0.223825	67.63
AC2M	0.5	2	1602	0.04005	96.74	12397	0.309925	94.20
AC3M	0.502	3	1630	0.04075	98.04	13083	0.327075	99.02
AC4M	0.501	4	1641	0.041025	98.90	12994	0.32485	98.54

Table A.3 – AAS results for reducing agent type and concentration effect
[2 M H_2SO_4; Time: 2 hours; Temperature: 40 ºC; Pulp density: 20 g/L]

Sample ID	LCO mass (gram)	Agent	Conc. (wt%)	[Li] (mg/L)	m_{Li} (gram)	% Li leached	[Co] (mg/L)	m_{Co} (gram)	% Co leached
RAC0	0.499	-	-	1136	0.02840	68.74	5147	0.1287	39.19
SMBS1	0.499	SMBS	1	902.9	0.02257	54.63	4293	0.1073	32.69
SMBS2	0.5	SMBS	2	902.1	0.02255	54.47	5957	0.1489	45.27
SMBS3	0.499	SMBS	3	1043	0.02608	63.11	6360	0.1590	48.43
SMBS4	0.501	SMBS	4	1061	0.02653	63.94	6401	0.1600	48.54
HP1	0.5	HP	1	1372	0.0343	82.85	10950	0.2738	83.21
HP2	0.5	HP	2	1628	0.0407	98.31	13050	0.3263	99.16
HP3	0.502	HP	3	1584	0.0396	95.27	12490	0.3123	94.53
HP4	0.499	HP	4	1649	0.04123	99.78	13120	0.3280	99.90

(**Notes**: SMBS = Sodium metabisulfite; HP = Hydro peroxide)

Table A.4 – AAS results for temperature effect
[2 wt% H_2O_2; 2 M H_2SO_4; Time: 2 hours; Pulp density: 20 g/L]

Sample ID	LCO mass (gram)	Temp. (ºC)	[Li] (mg/L)	m_{Li} (gram)	% Li leached	[Co] (mg/L)	m_{Co} (gram)	% Co leached
LTe25	0.503	25	1327	0.0332	79.65	10103	0.2526	76.31
LTe40	0.501	40	1594	0.0399	96.06	12670	0.3168	96.08
LTe60	0.499	60	1638	0.04095	99.11	13094	0.3274	99.70
LTe80	0.501	80	1647	0.0412	99.26	13023	0.3256	98.76

Table A.5 – AAS results for leaching time effect
[2 wt% H_2O_2; 2 M H_2SO_4; Temperature: 40°C; Pulp density: 20 g/L]

Sample ID	LCO mass (gram)	Leaching time (hours)	[Li] (mg/L)	m_{Li} (gram)	% Li leached	[Co] (mg/L)	m_{Co} (gram)	% Co leached
LT2h	0.501	2	1640	0.041	98.84	12947	0.3237	98.19
LT4h	0.503	4	1599	0.0399	95.98	13031	0.3258	98.43
LT6h	0.504	6	1605	0.0401	96.15	12895	0.3224	97.21
LT8h	0.5	8	1631	0.0408	98.49	12964	0.3241	98.51

Table A.6 – AAS results for pulp density effect
[2 wt% H_2O_2; 2 M H_2SO_4; Temperature: 40°C; Pulp density: 20 g/L]

Sample ID	LCO mass (gram)	Pulp density (g/L)	[Li] (mg/L)	m_{Li} (gram)	% Li leached	[Co] (mg/L)	m_{Co} (gram)	% Co leached
LS25	0.499	40	2712	0.0339	82.05	20816	0.2602	79.25
LS50	0.501	20	1595	0.0399	96.12	12861	0.3215	97.53
LS75	0.502	13.33	923	0.0346	83.27	7245	0.2717	82.25
LS100	0.5	10	681	0.0341	82.25	5107	0.2554	77.61

APPENDIX B – AAS RESULTS FOR SELECTIVE PRECIPITATION

Table B.1 – 1st try of selective precipitation
[Acid leaching: m_{LCO} = 1 gram; 4 wt% H_2O_2; 3M H_2SO_4; Time: 2 hours; Temperature: 60 ºC; Pulp density: 20 g/L]

V_{liquid}	pH (Sample ID)	$V_{NaOH\ 1M}$ added (mL)	$V_{Na2CO3\ 1M}$ added (mL)	$V_{filtrate}$ (mL)	[Li] (mg/L)	m_{Li} (gram)	% Li precipitated	[Co] (mg/L)	m_{Co} (gram)	% Co precipitated
50	1.37	0	-	50	1674.8	0.0820652	0	13330.4	0.6531896	0
49	2.01	258	-	253.2	265.4	0.06693388	18.44	2197	0.5540834	15.17
252.2	6.39	14.1	-	261.5	236.6	0.0616343	24.90	2288	0.596024	8.75
260.5	10.13	16.5	-	243	227.4	0.0550308	32.94	304.8	0.0737616	88.71
242	12.04	0.6	-	242.6	230.8	0.05576128	32.05	216.2	0.0522339	92.00
241.6	13.05	-	4	242	247.3	0.0595993	27.38	195.2	0.0470432	92.80
241	13.99	-	20	261	229.4	0.059644	27.32	179.1	0.046566	92.87

Table B.2 – 2nd try of selective precipitation
[Acid leaching: m_{LCO} = 1 gram; 4 wt% H_2O_2; 3M H_2SO_4; Time: 2 hours; Temperature: 60 ºC; Pulp density: 20 g/L]

V_{liquid}	pH (Sample ID)	$V_{NaOH\ 1M}$ added (mL)	$V_{Na2CO3\ 1M}$ added (mL)	$V_{filtrate}$ (mL)	[Li] (mg/L)	m_{Li} (gram)	% Li precipitated	[Co] (mg/L)	m_{Co} (gram)	% Co precipitated
50	0.99	0	-	50	1678.9	0.0822661	0	13317.1	0.6525379	0
49	2.02	203	-	249.5	225.4	0.0560119	31.91	2200	0.5467	16.22
248.5	6.17	17.1	-	260.5	273.8	0.0710511	13.63	2045	0.5306775	18.67
259.5	10.09	16.6	-	257	216.4	0.0553984	32.66	406.6	0.1040896	84.05
256	12.01	0.6	-	256.6	231.2	0.05909472	28.17	404.8	0.10346688	84.14
255.6	13.01	-	4	258	219.5	0.0564115	31.43	419.6	0.1078372	83.47
257	14.01	-	20	277	204.9	0.0565524	31.26	390.6	0.1078056	83.48

APPENDIX C – CALCULATIONS FOR EXPERIMENTAL FACTORS

- **Liquid volume**

$$V_{liquid} = \text{Liquid volume (mL)} = \frac{m_{Solid} \times 1000}{pulp\ density(\frac{g}{L})}$$

- **98% sulphuric acid volume**

$$V_{98\%H_2SO_4}(mL) = \frac{V_{liquid} \times C_M \times 98}{98\% \times \rho_{98\%H_2SO_4}(\frac{g}{mL})}$$

With $\rho_{98\%H_2SO_4} = 1.84\frac{kg}{L}$

And, density of different molar concentration H_2SO_4 at 20 °C as following **Table C.1**

Table C.1 – Density of sulphuric acid at different concentration (20 °C)

Concentration (M)	Density (g/mL)
0.25	1.02
0.5	1.03
1	1.06
2	1.12
3	1.18
4	1.23

- **70% nitric acid volume required to make 2 wt% HNO_3 for dilution before AAS analysis**

$$V_{70\%HNO_3}(mL) = \frac{V_{2\%HNO_3} \times \rho_{2\%HNO_3} \times 2\%}{70\% \times \rho_{70\%HNO_3}}$$

With $\rho_{2\%HNO_3} = 1.0078\frac{kg}{L}$; $\rho_{70\%HNO_3} = 1.42\frac{kg}{L}$

Table C.2 – Calculation for nitric acid dilution

$V_{2\%\ HNO_3}$ (mL)	$V_{70\%\ HNO_3}$ (mL)
200	4.5
250	5.5
500	10.5
1000	20.5

- **Amount of raw sodium metabisulfite required for acid leaching tests**

$$m_{RA}(g) = \frac{(V_{liquid} \times \rho_{acid} + m_{RA} + m_{LCO}) \times \%C}{Purity\ of\ chemical(\%)}$$

$$\Rightarrow m_{RA}(g) = \frac{V_{liquid} \times \rho_{acid} + m_{LCO}}{\frac{Purity\ of\ chemical(\%)}{\%C}} - 1$$

%C is the mass concentration of sodium metabisulfite in leaching solution.

Purity of SMBS is 97%

Major of leaching solution is sulphuric acid, hence, density of leaching solution is assumed as acid density at corresponding concentration.

Table C.3 – Mass of SMBS required in acid leaching tests
[m_{LCO} = 0.5g; Pulp density = 20 g/L; V_{liquid} = 25 mL; 2M H_2SO_4]

Mass concentration in leaching solution (%)	m_{SMBS} (g)
1	0.297
2	0.600
3	0.910
4	1.226

- **Volume of 30% hydro peroxide required for acid leaching tests**

$$V_{30\%\ H_2O_2} = \frac{V_{liquid} \times \rho_{acid} \times \%C}{30\% \times \rho_{30\%\ H_2O_2}}$$

%C is the mass concentration of hydro peroxide in leaching solution.

Density of 30% H_2O_2 ($\rho_{30\%\ H_2O_2}$) is 1.11 g/mL.

Major of leaching solution is sulphuric acid, hence, density of leaching solution is assumed as acid density at corresponding concentration.

Table C.4 – Volume of 30% H_2O_2 required in acid leaching tests
[m_{LCO} = 0.5g; Pulp density = 20 g/L; V_{liquid} = 25 mL; 2M H_2SO_4]

Mass concentration in leaching solution (%)	$V_{30\%\ H_2O_2}$ (mL)
1	0.84
2	1.68
3	2.52
4	3.36

APPENDIX D – ELECTROCHEMICAL TESTING RESULTS

Table D.1 – EIS result of recycled LCO

Re(Z)/Ohm	-Im(Z)/Ohm
21.2636	4.6802
22.7254	6.06039
24.1097	7.80036
25.8294	9.67227
28.0786	11.5372
30.7126	13.6295
33.5985	16.1874
37.1085	19.5015
42.4924	24.061
47.5251	29.6476
54.1105	36.6655
62.5524	45.1547
73.7136	54.914
87.7524	66.001
104.526	77.8202
126.305	89.5758
151.698	102.044
180.649	112.947
214.231	123.712
251.371	130.179
290.713	131.417
328.402	126.269
363.058	115.295
390.29	102.217
411.623	91.0557
427.118	82.6028
438.275	79.4014
449.276	87.2068
455.132	97.9476
466.933	120.303
470.995	161.047
481.148	215.021
506.2	301.486
514.808	443.905
511.385	620.119
537.94	887.419

Table D.2 – EIS result of commercial LCO

Re(Z)/Ohm	-Im(Z)/Ohm
18.6112	4.21302
19.3421	6.04693
20.6215	8.03335
22.568	10.1327
25.0036	12.587
27.8974	15.0566
31.2734	17.6301
34.8282	20.9644
39.3648	25.9048
44.5521	31.8048
51.6141	39.5437
60.6957	48.5461
72.5158	59.0697
87.4587	70.7185
106.182	83.2291
129.118	95.5208
156.594	106.978
187.09	116.172
222.166	123.923
256.534	128.046
292.711	129.061
327.241	127.782
360.849	123.249
389.644	117.563
414.443	114.224
436.082	114.615
458.595	122.157
481.548	130.909
513.64	154.755
542.351	179.417
586.301	208.318
627.66	250.857
668.929	294.75
718.448	349.336
781.598	432.745
827.174	572.176

Table D.3 – Cycling performance test result

Index	Discharge Specific Capacity (mAh/g)	
	Recycled LCO	Commercial LCO
1	6.7	120.6
2	2.5	124.1
3	1.2	121.9
4	0.8	119.5
5	0.6	117.6
6	0.5	115.2
7	0.5	112.9
8	0.5	110.9
9	0.5	109
10	0.4	107.2
11	0.5	105.6
12	0.4	104.2
13	0.4	102.9
14	0.4	101.5
15	0.4	99.9
16	0.4	98.3
17	0.4	97
18	0.4	95.9
19	0.4	94.9
20	0.4	94.1
21	0.4	93.4
22	0.4	92.8
23	0.4	92.3
24	0.4	91.3
25	0.4	90.4
26	0.4	89.4
27	0.4	88.7
28	0.4	88.2
29	0.4	87.3
30	0.4	87.4
31	0.4	87.1
32	0.4	86.5
33	0.4	85.4
34	0.4	84.9
35	0.4	85.1
36	0.4	84.9
37	0.5	85